

## **NOTE TO USERS**

**This reproduction is the best copy available.**

UMI<sup>®</sup>



# **Use of Cryofixation and a Novel Achilles Tendon Model in Determining the Effects of Tendinopathy on Failure**

by

**Rachelle Forsyth**

A Thesis submitted to  
the Faculty of Graduate Studies and Research  
in partial fulfilment of  
the requirements for the degree of  
**Master of Applied Science**

Ottawa-Carleton Institute for  
Mechanical and Aerospace Engineering

Department of Mechanical and Aerospace Engineering  
Carleton University  
Ottawa, Ontario, Canada  
September 2009

Copyright ©

2009 - Rachelle Forsyth



Library and Archives  
Canada

Bibliothèque et  
Archives Canada

Published Heritage  
Branch

Direction du  
Patrimoine de l'édition

395 Wellington Street  
Ottawa ON K1A 0N4  
Canada

395, rue Wellington  
Ottawa ON K1A 0N4  
Canada

*Your file* *Votre référence*  
ISBN: 978-0-494-60263-8  
*Our file* *Notre référence*  
ISBN: 978-0-494-60263-8

**NOTICE:**

The author has granted a non-exclusive license allowing Library and Archives Canada to reproduce, publish, archive, preserve, conserve, communicate to the public by telecommunication or on the Internet, loan, distribute and sell theses worldwide, for commercial or non-commercial purposes, in microform, paper, electronic and/or any other formats.

The author retains copyright ownership and moral rights in this thesis. Neither the thesis nor substantial extracts from it may be printed or otherwise reproduced without the author's permission.

**AVIS:**

L'auteur a accordé une licence non exclusive permettant à la Bibliothèque et Archives Canada de reproduire, publier, archiver, sauvegarder, conserver, transmettre au public par télécommunication ou par l'Internet, prêter, distribuer et vendre des thèses partout dans le monde, à des fins commerciales ou autres, sur support microforme, papier, électronique et/ou autres formats.

L'auteur conserve la propriété du droit d'auteur et des droits moraux qui protègent cette thèse. Ni la thèse ni des extraits substantiels de celle-ci ne doivent être imprimés ou autrement reproduits sans son autorisation.

---

In compliance with the Canadian Privacy Act some supporting forms may have been removed from this thesis.

Conformément à la loi canadienne sur la protection de la vie privée, quelques formulaires secondaires ont été enlevés de cette thèse.

While these forms may be included in the document page count, their removal does not represent any loss of content from the thesis.

Bien que ces formulaires aient inclus dans la pagination, il n'y aura aucun contenu manquant.

  
**Canada**

# Abstract

This thesis has three components: the testing of a new model of Achilles tendon degeneration and acute injury, the design of a study continuation, and the analysis of the dual cryogenic fixation assembly used to mechanically test the specimens in this study.

The major outcomes are that the thesis hypothesis that tendons with pre-existing degeneration recover their mechanical properties slower after injury compared to healthy tendons was disputed, that three new hypothesis have been made regarding humans Achilles tendons, and that the mechanical testing assembly requires improvement for further studies to take place.

The hypotheses are that: A) tendons recover mechanical strength early after injury by increasing the cross-sectional area, thus reducing stress, B) returning to load-bearing activity sooner increases the rate of mechanical strength recovery, and C) a mathematical model could correlate stress with optical density, and can be used to approximate the recovery of tendon strength.

In dedication to my wonderful family. To my father Bradley for being my endless inspiration, to my mother Pamela for her constant encouragement. To my brother Sean, sister Brittany and my loving partner Jeff. Without all of your support I would not be where I am today.

# Acknowledgments

I wish to acknowledge and thank the many people that have personally and academically made this thesis possible.

I thank my thesis supervisors and advisor for their guidance and constant support over the past two years. *Dr. Donald Russell* for his guidance and supervision throughout my schooling. I thank him for introducing me to the biomedical field and for giving me the opportunity to continue my education. *Dr. Guy Trudel* for supervising me and giving me the opportunity to work on this project. I thank him for his attention to detail, encouragement, and trust in my ability. *Dr. Hans Uthoff*, for being an advisor. I thank him for his support, feedback, and insight throughout the project.

This thesis would not have been possible were it not for the people who contributed to it. I thank: *Ying Nie* and *Marie-Eve Methot* for conducting the surgical procedures for this study. *Animal Care* for providing care for the animals in this study. *Dr. Rakhra* for his collaboration, for reading the MR and US images, for teaching me, and for readily meeting with me to answer questions and verify data. I would also like to thank the technologists, *Francine Mccullagh* and *Jane St. Germain* for obtaining the MR and US images for this study. *Dr. Laurent Dinh* and *Philippe St. Laurent* for their collaboration and for obtaining the bone mineral

density measurements for this study. *Nanthan Ramachandran*, *Philippe Poitras*, and *Andrew Speirs*, for training me on the use of the dual cryogenic fixation assembly, for always being available to answer questions, and for helping me out around the biomechanics laboratory.

I would like to thank the other members of the Bone and Joint research laboratory team whom I have grown very fond of over the past two years. *Ying Nie* for organizing the study and always being helpful when I had questions. *Elizabeth Coletta* for her encouragement and help with locating old papers and other reference material.

I would like to thank *Suzan Logie*, for teaching me to improve my writing skills and for dedicating so much of her time to help her students.

Most importantly I would like to thank my family for their endless support and encouragement: My Father *Bradley Forsyth* for his insight, encouragement, and feedback. Thank you for being available whenever I needed you and for dedicating so much of your time to help me. My Mother *Pamela Forsyth* for always believing in me and always doing the little things to help me out when I was really busy. These effort have not gone unnoticed. My amazing partner *Jeffrey Bruton* for encouraging me and doing whatever it took to help.

# Table of Contents

<b>Abstract</b>	<b>iii</b>
<b>Acknowledgments</b>	<b>v</b>
<b>Table of Contents</b>	<b>vii</b>
<b>List of Tables</b>	<b>xii</b>
<b>List of Figures</b>	<b>xiii</b>
<b>1 Introduction</b>	<b>1</b>
1.1 Motivation . . . . .	1
1.2 Outline . . . . .	3
<b>2 Background</b>	<b>5</b>
2.1 Medical Terminology . . . . .	5
2.2 Diagnostic Imaging . . . . .	7
2.2.1 Diagnostic Ultrasound Imaging (US) . . . . .	7
2.2.2 Magnetic Resonance Imaging (MRI) . . . . .	9
2.2.3 Dual Energy X-ray Absorptiometry (DXA) . . . . .	12
2.3 The Achilles Tendon . . . . .	13
2.3.1 Anatomy and Physiology . . . . .	13
2.3.2 Blood Supply . . . . .	16

2.3.3	Mechanical Properties of Achilles tendons . . . . .	17
2.3.4	Achilles Tendon Injuries/Tendinopathy . . . . .	20
2.3.5	Clinical Guidelines for the Treatment of Achilles Tendons after Major Injury or Surgical Repair . . . . .	22
2.4	The Use of the Rabbit Achilles Tendon in Research . . . . .	23
2.5	Mechanical Testing of Soft Musculoskeletal Tissue . . . . .	23
2.5.1	Methods of Tendon Fixation during Mechanical Testing . . . .	24
2.5.2	Cryogenic Fixation . . . . .	25
2.5.3	Compression Fixation . . . . .	27
2.5.4	Serrated Jaws . . . . .	28
2.5.5	Suturing . . . . .	29
2.5.6	Air-Dried . . . . .	30
2.5.7	Gluing . . . . .	30
<b>3</b>	<b>Problem Statement</b>	<b>32</b>
<b>4</b>	<b>Experimental Setup</b>	<b>35</b>
4.1	Experimental Design and Purpose . . . . .	35
4.2	Surgical Procedures . . . . .	37
4.2.1	Model of Ischemia Induced Degeneration (Groups 1 and 2) . .	37
4.2.2	Model of Full-Thickness Partial Tendon Injury in Tendons with Ischemia Induced Degeneration (Group 2) . . . . .	39
4.3	Collection and Storage of Specimens . . . . .	39
4.4	Imaging . . . . .	42
4.4.1	Diagnostic Ultrasound Imaging (US) . . . . .	43
4.4.2	Magnetic Resonance Imaging (MRI) . . . . .	43
4.4.3	Calcaneal Bone Mineral Density (BMD) . . . . .	45
4.5	Mechanical Testing . . . . .	45

4.5.1	Materials & Equipment . . . . .	45
4.5.2	Methods of Preparing and Mechanically Testing the Tendon Specimens . . . . .	46
4.5.3	Data Analysis . . . . .	52
<b>5</b>	<b>Experimental Results</b>	<b>53</b>
5.1	Imaging Results . . . . .	53
5.1.1	Diagnostic Ultrasound (US) Imaging . . . . .	53
5.1.2	Magnetic Resonance Imaging (MRI) Results . . . . .	54
5.1.3	Bone Mineral Density (BMD) Results . . . . .	56
5.2	Mechanical Testing Results . . . . .	56
5.3	Possible Correlation of Imaging Outcome Measures with Mechanical Properties . . . . .	58
<b>6</b>	<b>Discussion of Results</b>	<b>61</b>
6.1	Model 1 - Ischemia Induced Degeneration . . . . .	62
6.2	Model 2 - Ischemia Induced Degeneration and Acute Injury . . . . .	64
6.3	Comparison of Study Results to Test the Hypothesis of this Study . .	66
6.4	Correlation between Variables . . . . .	68
6.5	Comparison of Experimental Achilles Tendon Models with Human Achilles Tendons . . . . .	69
<b>7</b>	<b>Design for Continued Study/Future Work</b>	<b>71</b>
7.1	Hypothesis A . . . . .	72
7.2	Hypothesis B . . . . .	73
7.3	Hypothesis C . . . . .	74
7.4	Contributions and Future Work . . . . .	75

<b>8</b>	<b>Mechanical Testing Equipment Analysis</b>	<b>76</b>
8.1	Current Equipment . . . . .	76
8.1.1	Components of the Dual Cryogenic Fixation System . . . . .	76
8.1.2	Evaluation of Design . . . . .	79
8.2	Suggested Design Improvements . . . . .	82
<b>9</b>	<b>Conclusions and Future Research</b>	<b>85</b>
9.1	Experimental Study Conclusions . . . . .	85
9.2	Evaluation of Mechanical Testing Equipment . . . . .	87
9.3	Future Research . . . . .	87
	<b>List of References</b>	<b>89</b>
	<b>Appendix A Protocol: Mechanical Testing of Achilles Tendon</b>	<b>94</b>
A.1	Preparation . . . . .	94
A.1.1	Specimen preparation . . . . .	94
A.1.2	Dual cryogenic fixation assembly . . . . .	95
A.1.3	Thermometer set-up . . . . .	98
A.2	Specimen Fixing . . . . .	98
A.2.1	Freezing TOP fixation . . . . .	98
A.2.2	Mounting fixations . . . . .	99
A.2.3	Freezing BOTTOM fixation . . . . .	100
A.3	Mechanical Testing . . . . .	100
A.3.1	Maintaining the temperature of the cryogenic fixations while obtaining desired temperature gradient in the tendon . . . . .	100
A.3.2	Pre-loading . . . . .	101
A.3.3	Peak-load to failure . . . . .	101
A.4	Histology Preparation . . . . .	101

<b>Appendix B Experimental Summary Process Map</b>	<b>102</b>
<b>Appendix C Experimental Results</b>	<b>103</b>
C.1 Imaging Results . . . . .	103
C.2 Mechanical Testing Results . . . . .	107
<b>Appendix D Previous Healthy-Injured Study Results</b>	<b>110</b>
D.1 Imaging Results . . . . .	110
D.2 Mechanical Testing Results . . . . .	112
D.3 Correlations Between Imaging and Mechanical Results . . . . .	113

## List of Tables

1	Structure Appearances on MR Images . . . . .	11
2	Mean Ultrasound AP and TR Measurements . . . . .	54
3	Mean Cross-sectional Areas and Optical Densities . . . . .	55
4	Mean Bone Mineral Densities . . . . .	56
5	Mean Mechanical Properties . . . . .	57
6	Ultrasound Results for All Tendons . . . . .	103
7	Magnetic Resonance Imaging (MRI) Results for All tendons . . . . .	104
8	Bone Mineral Density (BMD) Results . . . . .	105
9	Ultrasound results for subset of valid tendons . . . . .	105
10	Magnetic resonance imaging (MRI) results for subset of valid tendons	106
11	Bone mineral density (BMD) results for subset of valid tendons . . .	106
12	Mechanical strength of Group 1 (Degenerated) tendons . . . . .	107
13	Mechanical strength of Group 2 (Degenerated & Punched) tendons .	108
14	Mechanical strength of contralateral tendons . . . . .	108
15	Previous Interval Study: Clinical imaging results . . . . .	110
16	Previous Longitudinal Study: Imaging results . . . . .	111
17	Previous Interval Study: Mechanical testing results . . . . .	112
18	Previous Longitudinal Study: Mechanical testing results . . . . .	112
19	Previous Study: Correlation between imaging outcome measures and mechanical measures 4 and 8 weeks after surgery [1] . . . . .	113

# List of Figures

1	Anatomical Planes and Orientation of the Body . . . . .	6
2	Ultrasound Image of a Rabbit Achilles Tendon . . . . .	8
3	MR Images of an Achilles Tendon . . . . .	12
4	The Achilles Tendon . . . . .	13
5	Foot Flexion . . . . .	14
6	Tendon Architecture . . . . .	16
7	Mechanical Properties of tendons . . . . .	18
8	Typical force vs. deformation curve for an achilles tendon and the regions	19
9	Distribution of Achilles tendon ruptures according to sports . . . . .	21
10	Cryofixation designed by Liggins <i>et al.</i> . . . . .	28
11	The plastic serrated jaw clamp designed by Cheung and Zhang . . . . .	30
12	Surgical Procedure . . . . .	40
13	Tendon Punch . . . . .	41
14	Acute punch injury in a rabbit Achilles tendon. . . . .	42
15	Tendon Box for Clinical Imaging . . . . .	44
16	The Rabbit Achilles Tendon Specimen . . . . .	47
17	Tendon Specimen fixed in Top and Bottom fixations . . . . .	48
18	Representative thermal profile of a rabbit Achilles tendon using the dual cryogenic fixation system seen in Figure 19. . . . .	49
19	Cryogenic Fixation System . . . . .	51

20	Sample of Load vs. Displacement curve during mechanical testing . .	52
21	Tendon Peak Load vs. T1 Weighted Optical Density . . . . .	58
22	Mean Tendon Stress vs. T1 weighted Optical Density . . . . .	59
23	Mean Tendon Stress vs. Proton Density Optical Density . . . . .	59
24	Mean Tendon Stress vs. Calcaneal Bone Mineral Density . . . . .	60
25	The complete Cryofixation setup . . . . .	77
26	Assembly of the bottom fixation . . . . .	78
27	Rabbit Achilles Tendon Specimen . . . . .	95
28	Fixation assembly Drawing Part 1 . . . . .	96
29	Fixation assembly Drawing Part 2 . . . . .	97
30	Process Map Summarizing the Experimental Procedures . . . . .	102
31	Load vs. displacement plot for Group 1 tendons . . . . .	107
32	Load vs. displacement plot for Group 2 (Degenerated & Punched) tendons . . . . .	108
33	Load vs. displacement plot for contralateral tendons . . . . .	109

# Chapter 1

## Introduction

The goal of this thesis was to conduct a preliminary study to evaluate a new model of Achilles tendon degeneration and acute injury. The results of this study led to areas of possible study continuations and a need for an improved method of mechanically testing tendon specimens. As a result, the dual cryogenic fixation assembly used to mechanically test the specimens in this study was evaluated and design improvements were recommended.

### 1.1 Motivation

The Achilles tendon is the most common site of tendonitis and tendon rupture in the lower limbs. The need for a means of predicting the risk of re-rupture of the Achilles tendon after injury has increased with the number of reported Achilles tendon injuries. There is limited human and experimental data available to predict the risk of re-injury and guide clinical management after major Achilles tendon injury or surgical repair.

Previous work, conducted by the Bone and Joint Laboratory at the University

of Ottawa [1], characterized the mechanical properties of rabbit Achilles tendons at various healing times after surgically creating a large central defect (acute injury) to healthy tendons. They also assessed the ability of imaging modalities (Magnetic Resonance Imaging (MRI), Ultrasound Imaging (US), Bone Mineral Density (BMD)) to predict the mechanical properties of rabbit Achilles tendons after injury. In this study, the mechanical strength of the rabbit tendons recovered as quickly as four weeks after surgery, with one tendon healing as fast as two weeks. This healing time was significantly faster than the clinically expected recovery time of humans, which can take up to 26 weeks. The imaging modalities, however, continued to show abnormal results (increased cross-sectional area and high MRI optical densities). The mean stress at peak load was noticeably lower as the cross-sectional area of the rabbit tendons increased, early after surgery. The difference in mechanical strength recovery, between the rabbit model and expected human results, was hypothesized to be attributed to the health of the tendon prior to injury. While the rabbit tendons in this study were healthy at the time of the surgically created defect, most human tendons are believed to suffer from degeneration prior to injury.

The exact cause of degeneration in Achilles tendons is unknown, however it is hypothesized that clinical tendons suffer from degeneration prior to acute injury causing rupture and that tendons with pre-existing degeneration are slower to normalize their mechanical properties. It was believed that hypovascularity in the tendons caused degeneration and therefore a reduction in the tendon strength.

Based on this hypothesis, a new experimental study was designed to account for degeneration due to ischemia (inadequate blood supply) followed by an acute partial tendon tear. The purpose of this study is to test a new model of Achilles tendon degeneration and acute injury. Two models are tested and compared in this study:

Model 1: degeneration due to ischemia, and Model 2: degeneration due to ischemia followed by an acute partial tendon tear.

## 1.2 Outline

The following chapter contains the background information necessary to understand the contents of this thesis. It contains information on medical terminology in regards to orientations, axis, and planes used to describe anatomy. It describes the modes of medical diagnostic imaging used in this study. A large portion of the background is dedicated to Achilles tendon anatomy, physiology, mechanical properties, injury, and treatment. The use of rabbit Achilles tendons in research is also included. The final portion of the background contains a literature review on methods of mechanically testing soft musculoskeletal tissue.

The problem statement follows the background and establishes the groundwork for the following chapters.

The experimental setup (Chapter 4) states the purpose of the study and describes the surgical procedures, imaging protocols, and mechanical testing methods used in the study.

The following two chapters (Chapters 5 & 6) include the results, discuss how they can be interpreted, and explore how they are relevant to the study. Based on these results, three new hypotheses were derived and are described in Chapter 7.

Chapter 8 evaluates the mechanical testing equipment and proposes design

improvements.

The key contributions of the thesis and recommendations for future work conclude the document (Chapter 9).

## Chapter 2

# Background

This chapter gives background on material relevant to this thesis:

- Medical Terminology
- Diagnostic Imaging: Ultrasound, Magnetic Resonance Imaging, and Dual Energy Absorptiometry
- The Achilles tendon: Anatomy, Physiology, Blood Supply, Mechanical Properties, Injury, and Clinical Treatment
- The use of the rabbit Achilles tendons in research
- Mechanical testing of soft musculoskeletal tissue

### 2.1 Medical Terminology

Three planes, illustrated in Figure 1, are used to describe the orientation of the body in medicine: The Frontal (or Coronal) Plane, Sagittal (or Lateral) Plane, and Axial (or Transverse) Plane.

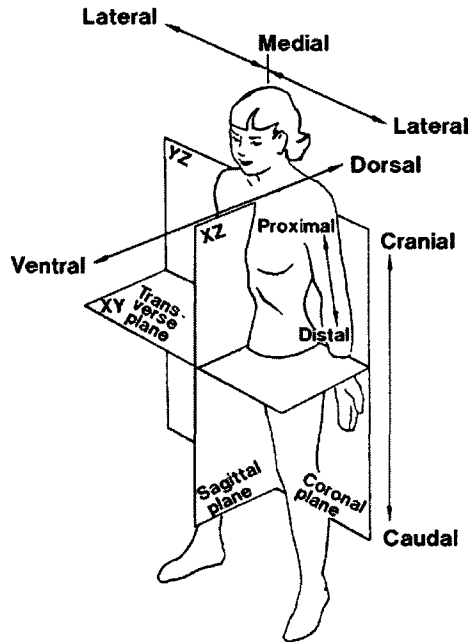


**Figure 1:** Anatomical Planes and Orientation of the Body, Obtained from NASA RO 1024 [2]

Relevant medical terms used to describe anatomy and location are defined below [3].

**Proximal** Closer to the origin of a body part or an attachment of a limb to the trunk of the body.

**Distal** Farther from the origin of a body part or an attachment of a limb to the trunk of the body.

**Anterior/Ventral** Toward the front of the body, in front, or at the front of the body

**Posterior/Dorsal** Towards the back of the body, behind, or at the back of the body

**Anteroposterior** From the front of the body to the back of the body

**Medial** On the inner side or towards the midline of the body

**Lateral** On the outer side or away from the midline of the body

**Medial-lateral** From the middle of the body outwards towards the sides

**Inferior** Below, away from the upper portion of the structure or body

**Superior** Above, towards upper portion of the structure or body

## 2.2 Diagnostic Imaging

Three imaging modalities have been used in this study: Ultrasound, Magnetic Resonance, and X-ray Imaging. This section includes information describing the technology involved in these modalities and their application in this study.

### 2.2.1 Diagnostic Ultrasound Imaging (US)

Ultrasonography is a useful diagnostic imaging tool that produces images, like the one in Figure 2, of anatomy sections (or slices), in multiple planes (Figure 1). The US machine consists of an US wave source, a transducer, and a computer. The US wave source emits short bursts of high frequency sound waves (1-10MHz) alternately, through the transducer, into the patient. When the sound waves hit a new boundary between media of different acoustic impedance ( $Z$ ), the sound waves are either absorbed, deflected, or reflected back into the transducer. The acoustic impedance of a structure determines the amount of sound energy that is transmitted or reflected at the structure's boundary. The impedance value is dependent on the tissue density and the velocity of sound ( $Z = \rho_{tissue} \times v_{sound}$ ) [4].

The reflected analog sound waves from the body tissue during imaging, are intermittently received by the transducer and digitalized. The digitized information is then converted into grey scale US images. Since the transducer alternates between

broadcasting sound waves and receiving the reflected waves, real-time imaging can be seen (Ex. the beating of a heart) on the monitor.

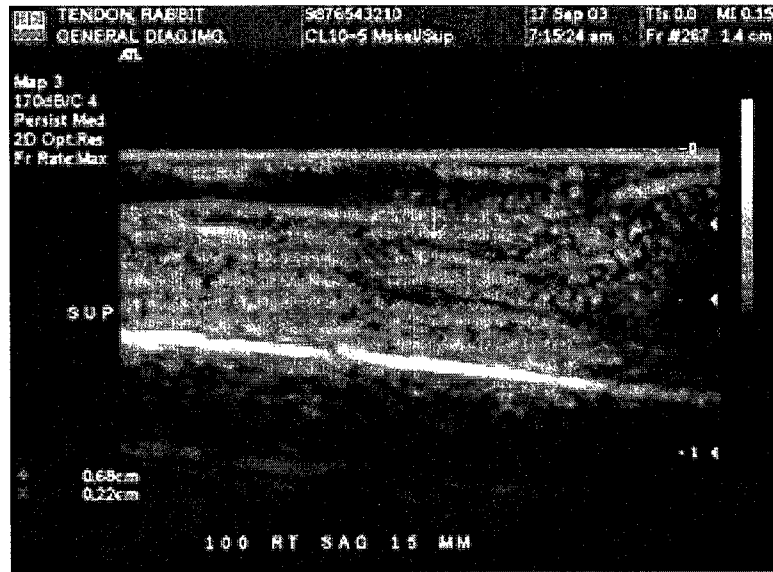


**Figure 2:** Ultrasound Image of a Rabbit Achilles Tendon. The arrow points to an observed defect in the tendon.

US imaging has been included in this study due to its advantages over MR imaging.

### Advantages to using US imaging

- Ability to take images in multiple planes
- Safe (No known harm biologically at diagnostic sound frequency levels)
- Painless
- Equipment is less expensive than MRI equipment
- Produces real time imaging (Not as important for this study)
- Portable

### Disadvantages to using US imaging

- Quality of images is operator dependent (Requires specific skill set to obtain good quality images)
- Contrast is poor

### 2.2.2 Magnetic Resonance Imaging (MRI)

Much like US imaging, Magnetic Resonance (MR) imaging is a means of displaying anatomy in different planes, at different slice thicknesses (1-10 mm). MR imaging takes advantage of the large quantity of hydrogen in the human body and its ability to be easily manipulated by magnetic fields. The protons in hydrogen are positively charged particles that are constantly spinning at a fixed frequency (called spin frequency). The small charge and spinning causes small magnetic fields to surround the protons. The north and south poles of these little proton magnets align themselves with the large magnet in the MRI machine. Short bursts of radio frequency waves, with frequencies equal to the spin frequency of the protons, are then broadcasted from the radio transmitter. The protons absorb the radio wave energy and begin to resonate (exchanging of energy between spin states). The broadcast of radio frequency waves is then discontinued and the energy in the protons begins to decay back to their normal state. During this decay period, the protons continue to resonate and broadcast their own radio waves. These radio waves are in turn detected by the radio wave receiver set to the same frequency as the proton spin frequency. The signal intensity detected by the radio wave receiver coil represents the quantity and location of the resonating hydrogen protons. A computer then interprets this information and outputs it in the form of grey scale MR images. The larger the number of hydrogen protons (higher density) the brighter the image (see Table 1 for typical structure appearances on MR images) [4]. The end result is a three-dimensional plot

of the anatomic slice being imaged. See Figures 3(a) and 3(b) on page 12 for examples.

The radio wave signal intensity reading is based on the number of hydrogen protons present when the radio wave signal was recorded. The radio wave signal can measure the T1 relaxation time, T2 relaxation time, or the proton density relaxation time (see definitions below). These times are defined by two parameters: echo time (TE) and repetition time (TR).

**Echo time (TE)** is the time between the radio frequency pulse and the MR signal sampling [4].

**Repetition time (TR)** is the time between two radio frequency pulses [4].

*T1 weighted* MR images are obtained by measuring the signal intensity early during the decay following discontinuation of the radio wave frequency. Short echo and repetition times are used to get T1 images. The purpose of T1 weighted images are more often for anatomical information because they are best at defining anatomy and have good spatial resolution. [4]

*Proton density* images depend primarily on the number of protons per unit of tissue (density of protons). These images are obtained with a long repetition time (TR) and short echo time (TE). Proton density images are usually similar to T1-weighted images. [4]

*T2 weighted* MR images are obtained when the signal intensity is measured late during the energy decay. Long repetition and echo times are used to get T2 images. These images tend to be used to analyze pathology since most pathology tends to show higher amounts of water and hydrogen and, as seen in Table 1, water shows up

very bright on T2 weighted MR images. [4]

**Table 1:** Structure Appearances on MR Images

Object	MRI		
	T1	PD	T2
Air	Dark	Dark	Dark
Water	Dark	Bright	Bright
Fat	Very Bright	Very Bright	Intermediate to Dark
Muscle	Dark	Dark	Dark

### Advantages to using MR imaging

- Multi-plane images
- Good contrast
- No known hazards
- Especially good for soft tissue injuries

### Disadvantages to using MR imaging

- Expensive
- Long scan times and confined imaging may cause claustrophobia and motion artifacts
- Limited availability
- No metallic objects can be present on or in the patient due to the large magnetic field.
- Requires special expertise to run the equipment and interpret the images

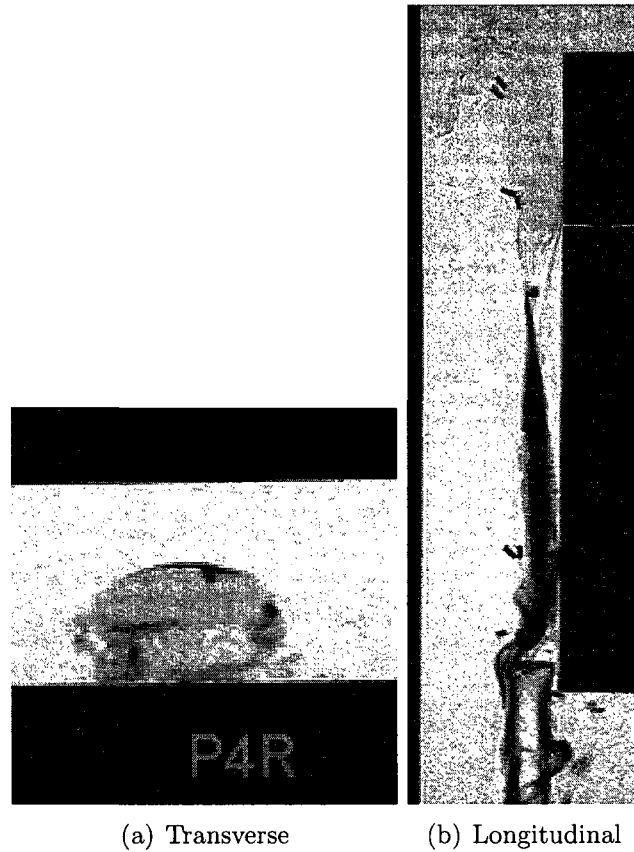


**Figure 3:** MR images of an Achilles tendon obtained for this study

### 2.2.3 Dual Energy X-ray Absorptiometry (DXA)

Dual energy x-ray absorptiometry (DXA) is the most commonly used means of measuring bone mineral density (BMD). Densities of bone are recorded by using two x-ray beams with different energy levels aimed at the bone in question. One beam is absorbed by soft tissue and the other by bone. The absorption of the soft tissue surrounding the bone is subtracted and the remaining beam absorption is the BMD measurement [5]. The BMD obtained is actually an areal density, as it is calculated using the area of the bone rather than the volume. The missing dimension is the thickness of the bone. The areal BMD is however, a good indicator of density and is often used for comparison between studies [6] [7]. DXA is also inexpensive and easily

accessible which are two very important factors when conducting a study.

## 2.3 The Achilles Tendon

This section provides the anatomy and physiology of the Achilles tendon, the pathology of Achilles tendon degeneration and repair, and the current guidelines dictating the clinical management of Achilles tendons after major injury or surgical repair.

### 2.3.1 Anatomy and Physiology

The Achilles tendon connects the two calf muscles (gastrocnemius and soleus) to the heel bone (calcaneus) (Figure 4). The length of the average tendon in men is 68 mm and in women is 60 mm [8].

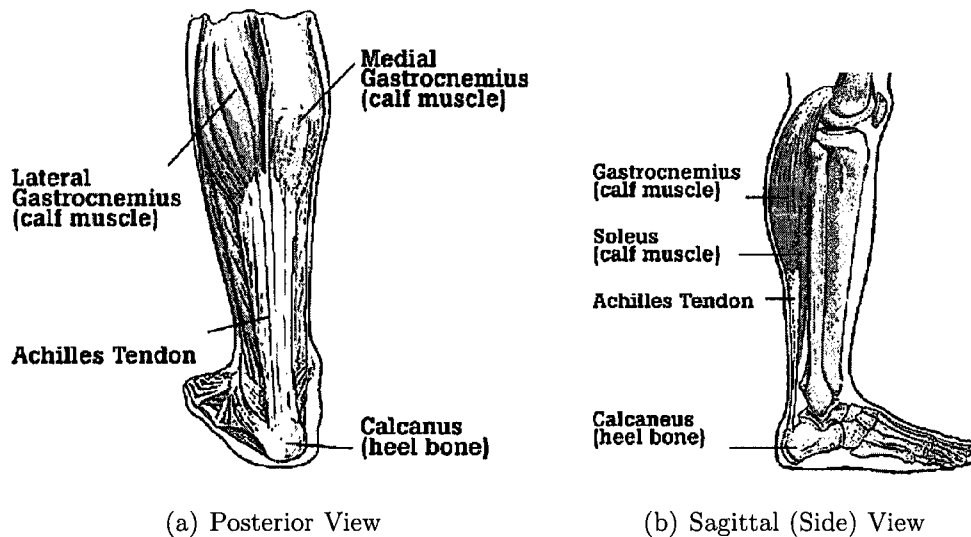


**Figure 4:** The Achilles tendon. Connects the calcaneus (heel bone) to the gastrocnemius and soleus (calf muscles). (Figures obtained from [www.achillestendon.com](http://www.achillestendon.com), 2009, [9])

The Achilles tendon transmits load and acts as a shock absorber, an energy storage device, and a passive elongation resistor. The function of the tendon is to transfer the load created by the muscles to the heel bone, pulling on it like a lever, to allow flexion of the foot (plantar/toe down motion illustrated in Figure 5). This motion of the foot allows a person to walk, stand on one's toes, jump, etc. Achilles tendons are subjected to very high loads and can withstand up to 12.5 times one's body weight [10].

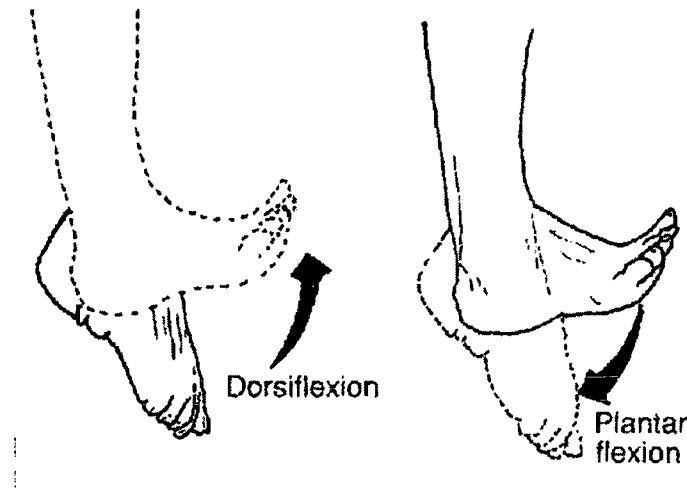


**Figure 5:** Foot Flexion

An area of twist along the length of the tendon produces an area of increased stress and reduced vascularization, which is the most common site of injury. Achilles tendons are wide and thin at the calcaneal insertion and gradually become smaller in cross-sectional area at the center where the tendon becomes more rounded before branching back out to meet the calf muscles. As the tendon descends towards the calcaneus, it twists about  $90^\circ$  externally (above the soleus attachment). This spiral causes the fibers coming from the soleus muscle to insert medially, and from the gastrocnemius to insert laterally into the posterior portion of the calcaneus [8]. This twist results in elongation and elastic recoil which aids in tendon energy storage.

The tendon is made up of an extracellular matrix (ECM) consisting of collagen (30%), elastin (2%), proteoglycans, cells (such as tenocytes) and water (68%). These components give the tendon its unique mechanical properties [10].

**Collagen fibers** are assembled from collagen molecules secreted by the cells. Collagen type I is the collagen present in tendons. The number, size, and orientation of the collagen fibers in the tendon determine the mechanical strength of the tendon. The orientation of the fibers are based on the range of motion and load requirements of the tendon.

**Elastin fibers** are formed from a coiled molecule called elastin. These fibers give the tendons flexibility.

**Proteoglycans** are proteins that have one or more glycosaminoglycan side chains (GAG). These GAGs are hydrophilic and retain very large volumes of water. As a result, proteoglycans help maintain hydration in the tendons [11].

**Tenocytes** are cells that secrete collagen molecules which aggregate to form collagen fibrils.

Tendons are made up of a complex hierarchy structure, illustrated in Figure 6, that causes tensile strength and stiffness. *Tropocollagen* is the basic collagen unit and is composed of three polypeptide chains. Tropocollagen aggregates to form *microfibrils*. The microfibrils then form collagen fibrils which make up collagen fibers. Groups of collagen fibers form fascicles which are surrounded by a connective tissue sheath, the *endotenon*. This sheath contains the tendon's intra-tendinous blood, lymphatic vessels, and nerves. The fascicles bundle together and are surrounded by the *epitenon*. Several of these fascicle bundles form the tendon which is surrounded

by a final sheath called the *paratenon*. [10] [11].

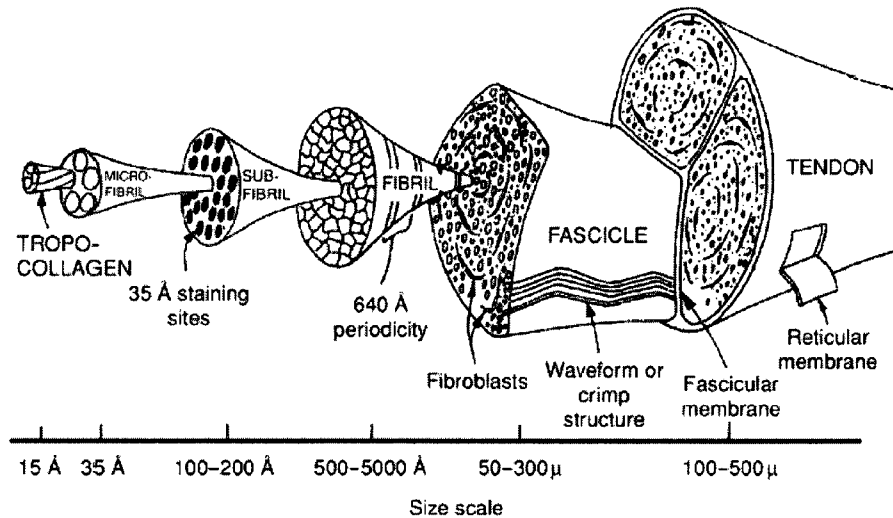


**Figure 6:** Hierarchy of tendon structure and associated size scales. [11]

The structure and tendon composition changes at the osteotendinous (tendon-bone) and musculotendinous (muscle-tendon) junctions to ensure sufficient force transfer and reduce risk of tear. At the osteotendinous junction the tendon tissue converts to fibrocartilage and then calcified fibrocartilage before insertion into the bone. The musculotendinous junction is considered the growth plate of the muscle; in this region the tendon elongates [10].

### 2.3.2 Blood Supply

There are three regions that supply blood to the tendon:

1. **Musculotendinous junction** The blood is supplied by small arteries that branch and supply both the muscle and the tendon through superficial vessels in the surrounding tissue [10].

2. **Length of the tendon** The paratenon is the main supply to the middle portion of the tendon. Within the paratenon are small blood vessels that run transversely towards the tendon and branch off into smaller vessels before running parallel to the length of the tendon [10].
3. **Osteotendinous junction** Vessels from the this region supply one third of the lower end of the tendon [10].

### 2.3.3 Mechanical Properties of Achilles tendons

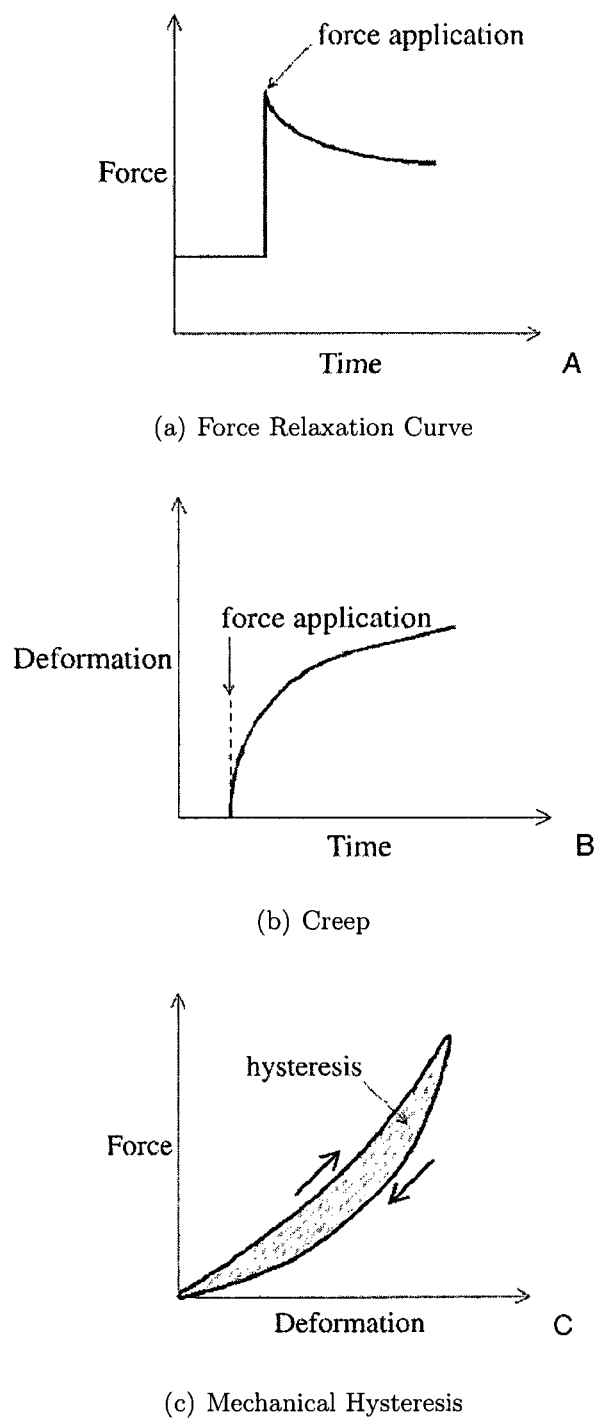
The collagen fibers in the tendon are crimped like springs causing the collagen fibers and interfiber matrix to possess viscous properties. As a result, tendons exhibit force-relaxation, creep, and mechanical hysteresis [11].

**Force relaxation** is when the force required to maintain a constant deformation decreases over time, this is illustrated with the force-time graph in Figure 7(a).

**Creep** is when a constant force causes slow permanent deformation, this is illustrated with a deformation-time graph in Figure 7(b).

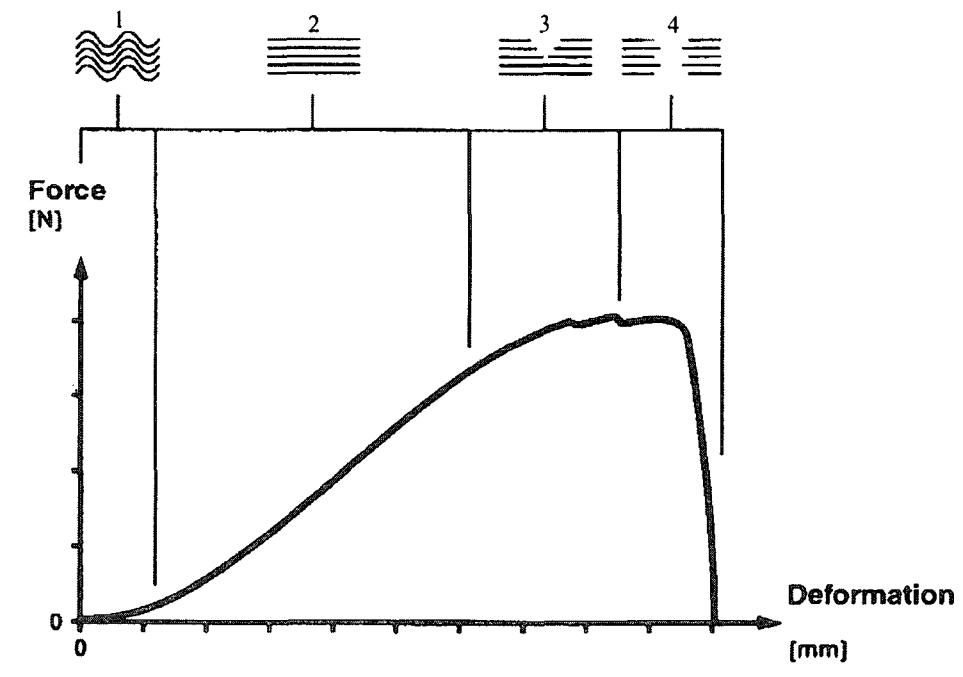
**Mechanical hysteresis** is when the response of the tendon to a force is not only dependent on the force but also dependent on historical loading on the tendon, this is illustrated in Figure 7(c).

Figure 8 illustrates a typical force-displacement (deformation) curve for an Achilles tendon. Four regions exist along this curve:



**Figure 7:** Mechanical Properties of tendons. a) shows a typical force relaxation curve, b) illustrates creep, c) demonstrates hysteresis. [12]

1. **Toe Region** is the initial concave region of the curve. In this region the collagen fibers are elongating reducing the crimp angle of the collagen fibers at rest. In this region the stretching does not exceed the tendon's elastic region (stretching  $< 2\%$ ).
2. **Linear Region** is when the crimp is completely straightened and the collagen fiber stiffness remains constant as a function of elongation. During this region the collagen fibers are being stretched (stretching  $> 2\%$ ).
3. **Beginning of Fiber Failure** micro-tears in the tendon begin to occur.
4. **Complete Failure** occurs when all of the fibers in the tendon fail and a sudden decrease in force occurs.



**Figure 8:** Typical Force vs. Deformation curve for Rabbit tendon and illustrated regions [12]

## **Activity and its affect on the mechanical properties of tendons**

**Physical Activity** Exercise has shown to have positive effects on the mechanical properties of tendons. Some benefits include increases in stiffness, ultimate strength, and energy-to-failure. These changes result in improved mechanical properties. [12] [13] [14]

**Disuse** has been reported to cause an undesirable decrease in stiffness, ultimate strength, and energy-to-failure. These changes are a result of changes in the tendon's material properties and atrophy. The changes in tendon material properties are associated with increased collagen turnover and an increase in nonuniform orientation of collagen fibrils. [12] [13] [15] [16].

### **2.3.4 Achilles Tendon Injuries/Tendinopathy**

Achilles tendon injuries (tendinopathy) can range from degenerative changes to complete rupture of the tendons [8].

**Tendinosis** is a structural degeneration of the tendon. Typical symptoms are pain and inflammation; however it does not always present with symptoms. It results in weakened tendon strength and causes the tendon to be at higher risk of rupture if left untreated. [8] [17] [18]

**Paratenonitis or Achilles tendonitis** is the inflammation of the peritendinous tissue, often caused by repetitive strain or over-use. [8] [18]

**Tear** is a partial disruption of the collagen fibers.

**Rupture** is complete disruption of the collagen fibers. Surgical intervention is required in cases of complete rupture. [8] [18]

## Epidemiology

The incidence of complete Achilles tendon rupture has increased over the past few decades. [19]

Achilles tendon ruptures are more common in males, although this is believed to result from the greater prevalence of men in sports. [19]

The majority of Achilles tendon ruptures are related to sports that consist of jumping and sudden acceleration (44% to 84%) [19]. Figure 9 shows the distribution of Achilles tendon ruptures according to sports.

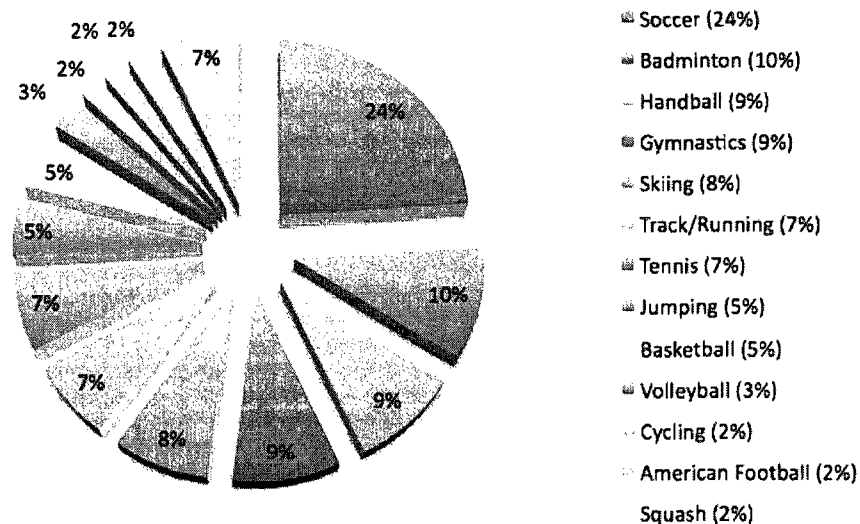


**Figure 9:** Distribution of Achilles tendon ruptures according to sports. The data for this figure was obtained from various studies cited by Paavola *et al.* [20].

### **2.3.5 Clinical Guidelines for the Treatment of Achilles Tendons after Major Injury or Surgical Repair**

The clinical management of acute Achilles tendon rupture is primarily dependent on the preference of the surgeon and the patient, however, severity of the injury plays a big role. Depending on the severity of the injury tendons may be treated non-operatively or operatively. Non-operative treatment methods are generally exhausted before resorting to operative treatment.

In both cases, the tendons are immobilized. Non-operative treatment consists of immobilizing the tendons in a plaster cast for 6 to 10 weeks. Post-operative care also consists of applying a plaster cast for 6 weeks. The foot is placed in plantar flexion at varying angles throughout this time, with flexion maximum early after surgery and decreased in increments after. Patients then gradually reintroduce weight bearing 8 to 10 weeks after cast or surgery. Initial stages of treatment focus on reduction of pain and inflammation, and increasing range of motion of all associated joints (Ankle, Hip, and knee).

Patients are normally able to return to normal activity 16 weeks post-operative. [19] [21] [22]

## **2.4 The Use of the Rabbit Achilles Tendon in Research**

The use of animal models enables in-depth invasive analysis of tendons and their microstructure. Invasive analysis provides researchers with an advanced comprehension of the aspects of tendinopathy, supports clinical data, and allows for testing of hypotheses [23].

The rabbit is used in this study to investigate Achilles tendon degeneration and acute injury. The rabbit is frequently used in Achilles tendon research due to its good availability and size. These tendons are large enough for mechanical testing and small enough for histological assessment [15] [16] [24] [25] [26].

Rabbit Achilles tendons are suitable for human research because their cellular and tissue physiology approximates that of humans [27].

## **2.5 Mechanical Testing of Soft Musculoskeletal Tissue**

Tendons mechanically serve the musculoskeletal system and therefore knowledge of their mechanical properties are crucial to clinical treatment. The mechanical properties obtained contribute to the knowledge of Achilles tendons and serves as a means of comparing healthy tissue to injured tissue.

The only way to measure the mechanical strength of tendons is to mechanically

test them *in-vitro* (outside the body). This section defines mechanical testing, lists the common issues with mechanically testing tendons, discusses the possible methods of rigidly fixing the tendons for testing, and makes the argument that a dual cryogenic fixation system yields the most accurate mechanical results.

For the purposes of this study, mechanical testing refers to the application of a uniaxial tensile load to biological tissue to obtain the material's mechanical properties. The mechanical properties of interest are the tissues peak tensile load to failure and the strain during loading. The peak tensile load to failure is defined as the maximum achievable load tolerated by the specimen before failure and the strain is measured to be the deformation, in this case elongation, of the specimen during loading.

### **2.5.1 Methods of Tendon Fixation during Mechanical Testing**

To apply the tensile load, both ends of the specimen must be rigidly fixed to the loading frame. An ideal fixation will firmly hold the ends of the specimen without causing damage or allowing slippage at the fixation. Damage to the specimen alters the mechanical properties of the material and slippage at the fixation yields inaccurate strain results. Tendinous tissues are aqueous, deformable, and display viscoelastic properties under tension causing the tendon-fixation interface to be low friction and making proper fixation difficult. There is no standard method of fixing soft tissue for mechanical testing, however, cryogenic, compression, serrated, air-dried, and glued fixation techniques have attempted to overcome these difficulties.

Cryofixation is used in this study as it has proven to minimize fixation issues, allow for isolation of the tendon, and yield more accurate results. The following sections describe the advantages and disadvantages of the various fixation techniques.

### 2.5.2 Cryogenic Fixation

The fixation device used in this study uses cryogenic techniques. Cryogenic techniques were first introduced by Riemersma and Schamhardt to overcome some of the problems previously described with tendon mechanical testing [28]. These techniques take advantage of the high water content of the tendon tissue by freezing it to achieve stable fixation during tensile loading. Riemersma and Schamhardt tested 14 digital flexor tendon equine specimens without apparent slippage using cryogenic techniques. These techniques have since been used by other scientist to evaluate the mechanical properties of tendons [15] [28] [29] [30] [31] [32] [33] [34] [35] [36] [37] [38] [39].

Mathews et al. analyzed the mean surface strain of both frozen and unfrozen techniques [40]. They concluded that freezing tendon ends before clamping reduced pre-loading of the surface tendon fibres, which prevents slippage and allows for larger gripping forces without deformation. Freezing also enables uniform straining of the surface and core fibres [40]. Mathews et al. did not however, investigate transitional thermal zones created by freezing which may alter the mechanical properties of the specimen rendering inaccurate results.

Both Rincon and Schamhardt [30] and Ramachandran et al. [31] conducted thermal analyses of the specimen tissue during fixation. Both studies showed steep temperature gradients along the specimens with the midsection at room temperature [30] and at body temperature (approx. 36°C) [31]. Rincon and Schamhardt found that the temperature of the specimens was not thermally affected by the frozen

clamp beyond a distance of 3 cm from the fixation. Ramachandran et al. added a heater and insulating plates to their final setup to ensure a steep temperature gradient and body temperatures at the midsection of the tendons. Both studies showed accurate mechanical results and transitional thermal zones did not prove to be an issue.

Rincon and Schamhardt classified two types of cryogenic fixation techniques: cryoclamps and cryofixations [30].

### **Cryo-clamps**

Cryoclamp techniques mechanically clamp the frozen ends of the specimen [30]. The freezing of the ends causes rigidity of the specimen eliminating complex strain distributions through the cross-section of the specimen [40]. Cryo-clamp techniques have been successfully used by investigators of biomechanical properties [28] [34] [35] [36] [37] [38] [39] [40] [41] [42].

The most recent and promising cryo-clamp results have resulted from Lepetit et al. [34]. They designed a simple inexpensive cryogenic holder that allows for preparation of samples in three minutes. The holder freezes the ends of the specimen while maintaining ambient temperature at the midsection. This six piece holder is built out of celeron which is a bakelite cloth with very low thermal conductivity (0.26 W/mK) and is easily processed.

### **Cryofixations**

Cryofixation freezes the tissue ends in a medium, such as saline solution, and requires no compressive clamping. Rincon and Schamhardt designed the first promising

cryofixation clamp [30]. The design consists of two solid aluminum blocks with a half cylindrical hole machined along one side of each. These aluminum blocks were submerged in liquid nitrogen and then placed around a core chamber where the tendon was wrapped around a stainless steel rod and sutured to itself. Water was then poured into the core chamber where it instantly froze securing the specimen ends. Rincon and Schamhardt tested sixteen cadaveric patellar ligament specimens using this cryofixation and measured an overall average failure load of 2219 N. All failures occurred in the midsection of the specimens and no slippage or rupture at the ends fixed by the cryofixation were observed. Cooling the aluminum block in a bath of liquid nitrogen simplifies handling of the freezing agent and avoids direct contact with the midsection of the specimen. Cast aluminum is easily machined and has a high heat capacity (0.88 kJ/Kg K at 20°C).

Liggins et al. compared cryo-clamps to cryofixation and found that cryofixation yielded much better results [29]. Their design, see Figure 10, created the cryofixation by wrapping the patellar tendons around a steel cable and suturing through the tendon and cable, linking them together. A plastic tubing was snugly fit around the tendon-cable attachment, which allowed for the containment of liquid nitrogen and water. Liquid nitrogen and water were poured into the tubing, freezing the tissue in the water. The average peak load to failure achieved was approximately 6 kN with this method.

### **2.5.3 Compression Fixation**

Original fixations use metal plates to apply a compressive force to increase the coefficient of friction at the specimen-clamp interface and better grasp the specimen [33] [42] [43] [44] [45]. These plates are often lined with different layers of

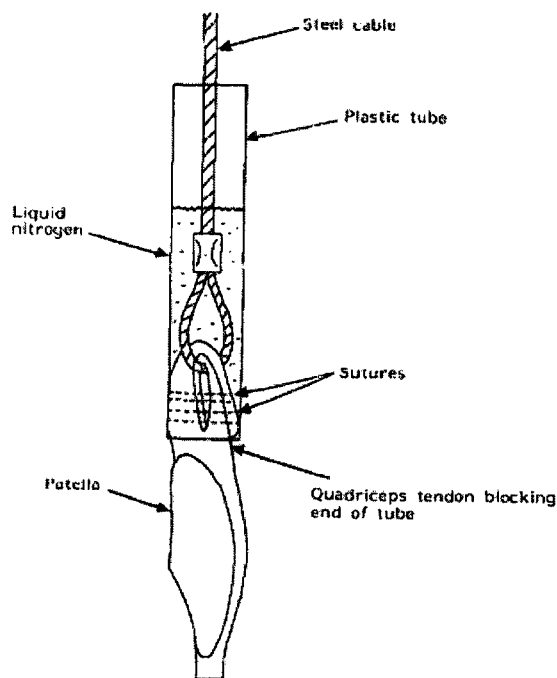


**Figure 10:** Cryofixation designed by Liggins *et al.* [29].

abrasive textiles and paper that increase the friction at the clamps. Pneumatics and hydraulics may also be used to maintain a constant clamping force on the specimen during loading [33]

The major issue with compressive fixation is that compression noticeably deforms the clamped regions of the specimen causing damage to the collagen fibres. This damage degrades the mechanical properties of the specimen [46].

#### 2.5.4 Serrated Jaws

To increase friction and gripping capabilities of clamps [33] [46] metal plates have been adapted with serrated faces. These clamps, like the one in Figure 11 are called serrated jaws. The matched serrated surfaces significantly increase the frictional force applied to the specimens, but also introduce stress concentrations. These stress

concentrations weaken the specimen and often cause premature rupture at the clamp.

Cheung and Zhang [46] designed the most recent serrated jaws with improvements, although they are still inferior to cryofixation. Their plastic serrated jaw clamp was tested through the tensile testing of bovine tendons. The maximum tensile load achievable before slippage was 3000 N. These results were an improvement from previous serrated clamp designs however, the peak load to failure attainable before slippage was still lower than results found using cryogenic type techniques. The clamp's success was attributed to the smooth edges of the jaw border and indentations of the plastic rack along with the relatively soft plastic material. These characteristics prevent cutting of the tendon fibres. However, permanent deformation and damage of the tendon still occurs with the tendon conforming to the shape of the serrated clamp. The high compression clamping also causes direct pre-strain of the tendon fibres at the surface of the tendon. This pre-strain results in altered mechanical properties of the tendon due to the fact that the surface fibres are pre-stretched causing an initial loading response. This initial loading response stiffens the tendon causing unfrozen tendon specimens to be stiffer than frozen tendons at the beginning of mechanical testing.

### **2.5.5 Suturing**

Wrapping the end of the specimen around a cable and suturing it to itself for mechanical testing was attempted by Liggins et al. [29]. Their study compared three means of clamping the tendon-muscle insertion for mechanical testing: A) Suturing the specimen to a steel cable; B) Freezing the suture end; and C) freezing the sutured end in water. The first technique which involved only sutures yielded the worst results. The cause of this is believed to be that suturing techniques are limited to the strength

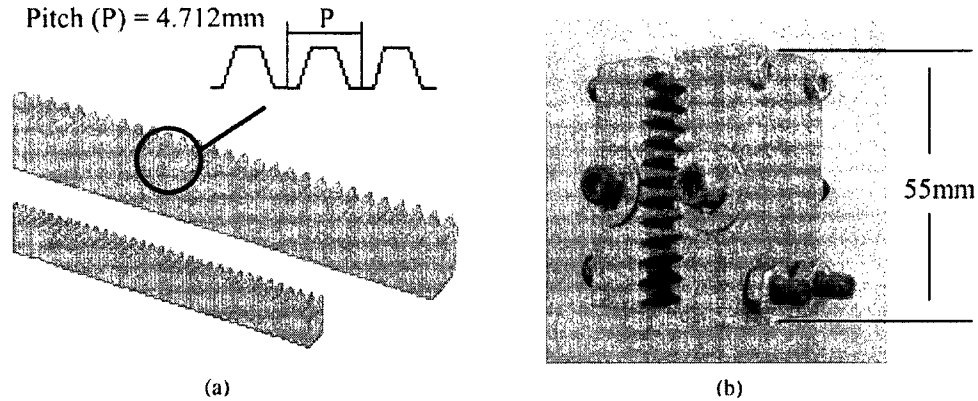


**Figure 11:** The plastic serrated jaw clamp designed by Cheung and Zhang [46].

of the sutures. The third technique, a form of cryofixation, resulted in the best results.

### 2.5.6 Air-Dried

The ends of the tendon are air-dried, creating a dry clamping area with higher surface resistance with reduced viscoelastic properties. The results obtained using this technique may not accurately represent the properties of live tissue because the properties of the tissue have been altered. Air-dried ends create transition zones where the mechanical properties are altered [33]. In particular, water is a key component of tendon mechanical properties and loss of water affects these properties. Results obtained using air-dried techniques are believed to be a combination of dried and fresh tissue properties and are therefore not a suitable representation of fresh tissue mechanical properties [33]. The process is also time consuming.

### 2.5.7 Gluing

Gluing the ends of a specimen to the grip is only suitable for thin specimens as adhesion to the outer surface of the tendon causes high shearing between the outer

surface and the core of the tendon. Less load is applied to the core of the tendon than the outer surface, causing very complex load distributions through out the thickness of the specimen [33]. Thin slices of the specimen could be used however, the mechanical properties of the tendon are greatly influenced by the structure of the tendon and therefore the entire specimen is required for accurate mechanical testing.

## Chapter 3

# Problem Statement

The incidence rate of Achilles tendon injury and rupture is increasing and necessitating a better understanding of the recovery mechanisms. Current clinical guidelines for return to activity after acute injury or surgical repair are conservatively based on clinical experience alone. This is because the strength to failure of Achilles tendons cannot be measured clinically. It would be ideal to be able to determine the mechanical weakness after large acute tear, the risk of progression of a tear to rupture, and the level of activity possible without risk of re-rupture after repair. Clinical imaging such as diagnostic ultrasound (US), magnetic resonance imaging (MRI), and bone mineral density (BMD) are non-invasive modalities that are currently investigated as a base for tendon treatment guidelines. If a means of determining the mechanical properties of Achilles tendons was discovered, prediction of the risk of rupture would be possible. To investigate the potential of using imaging tools to predict the mechanical properties of Achilles tendons, actual mechanical results must be compared to imaging results. Since this is not possible clinically, animal models must be used.

The Bone and Joint Research Laboratory at the University of Ottawa previously investigated the possibility of using imaging to predict Achilles tendon vulnerability

to rupture. The purpose of their study was: to characterize the mechanical properties of Achilles tendons at various healing times after surgically creating a large central defect in the tendons; and to assess the ability of MR, US, and BMD imaging modalities to predict the mechanical properties of rabbit Achilles tendons after injury. The end goal of the study was to produce experimental data to guide clinical management after large Achilles tendon injuries or surgical repair.

Thirty-eight adult female New Zealand white rabbits (approx. 4.5 Kg) were subjected to full thickness central tendon defects. All contralateral legs were used as controls. The study was broken into two parts: 1) interval study, where groups of ten rabbits were euthanized either immediately after surgery, or 4, or 8 weeks after surgery, 2) longitudinal study, where a single rabbit was euthanized each at 0,1,2,4,6,8,10, and 16 weeks after surgery. The purpose of the longitudinal study was to assess any possible trends that may be missed between 0, 4, and 8 weeks in the interval study. US, MRI, and BMD images were taken of all tendons in the study. The US images were used to measure any changes in cross-sectional size between healing times. The MR images were also used to measure changes in size and also measured T1 weighted, Proton Density, and T2 weighted optical densities. BMD images measured the bone mineral density of the whole calcaneal bone attached to each tendon. After imaging the tendons were tested mechanically, using a dual cryogenic fixation assembly, for peak load to failure, stress, and stiffness. Peak load to failure is the best indicator of the strength of the tendons. All of the data was then tested statistically for significant differences and correlations between variables.

Observed results showed an unexpected recovery of mechanical strength with changes in cross-sectional area and stress. They found that the peak load to failure had recovered by 4 weeks and possibly as fast as 2 weeks (according to the

longitudinal study). These results suggest that this model of Achilles tendon injury is quick to return its maximum mechanical tensile strength. Despite the recovery of peak load to failure, the mean stress decreased and the cross-sectional area increased right after injury. This suggests that early after injury, a large amount of new extracellular matrix material (mostly collagen fibers) with lower mechanical strength is placed in the site of injury to recover the peak load to failure. The quick recovery of the peak load to failure in this study was somewhat inconsistent with clinical results and it was hypothesized that the cause was that the acute injury was done on healthy tendons. In reality, the majority of middle-aged human tendons have suffered from some form of previous injury and quite commonly suffer from pre-existing degeneration.

The exact cause of degeneration in Achilles tendons is unknown, however, it is hypothesized that degeneration occurs prior to acute injury predisposing tendons with pre-existing degeneration to slower normalization of their mechanical properties. Hypovascularity can cause degeneration and therefore reduction in the tendons strength. Based on this hypothesis a new experimental study was designed to account for degeneration due to ischemia followed by an injury. This study was designed to test this new model of Achilles tendon degeneration and acute injury. Two models were tested and compared in this study: Model 1: degeneration due to ischemia (Strangulation), and Model 2: degeneration due to ischemia followed by injury (Strangulation & Punch). Model 1 was created as an experimental control and allowed for testing of degeneration due to ischemia.

The remainder of this document contains the experimental setup, the results, a discussion of these results, and an evaluation of the mechanical testing equipments used in this study.

## Chapter 4

# Experimental Setup

This chapter describes the setup and methods used to create and test two new models of Achilles tendon pathology. The following sections explain the experimental design and purpose, the surgical procedures conducted to obtain our models, the imaging protocols, the mechanical testing procedures, and the methods used to analyze the results of the imaging and mechanical testing.

### 4.1 Experimental Design and Purpose

Dr. Guy Trudel and his team at the Bone and Joint Research lab at the University of Ottawa, created the experimental design for this study.

Ten adult female New Zealand white rabbits (*Orytolagus cuniculus*)(Charles River Canada, Saint-Constant, QC, Canada), each of which weighed approximately 4.0 kg, were used to create two Achilles tendon models. A variety of animals have been used to model and research Achilles tendon injury, surgery, and repair, however, the rabbit was selected for this study because its Achilles tendon is large enough for mechanical testing and small enough for histological assessment. All procedures

conducted were in accordance with the ACSM animal care standards and approved by the Ottawa University Animal Care Committee.

All ten rabbits underwent two surgeries. The purpose of the first surgery was to create a form of tendinopathy by cutting off the blood supply to the midsection of the tendon. Eight weeks later, the second surgery was performed where the blood supply was returned to the tendons. Half of the rabbits underwent an additional surgical procedure, where a full thickness partial tendon tear was created to simulate injury. From these surgeries, two Achilles tendon models were created: 1) Model of ischemia induced degeneration (Group 1 - Strangulated); and 2) Model of injury in a tendon with degeneration (Group 2 - Strangulated & Punched).

Two and four weeks after the second surgery, the tendons were harvested, imaged and mechanically tested, so that the models could be compared and validated. The images were used to analyze changes in size, optical density, and bone mineral density. These properties were also compared to the strengths of the tendons, measured during mechanical testing, in order to investigate potential correlations. Please see Appendix B for a detailed process map of the experimental procedures.

The following sections include an explanation of the surgical procedures, specimen collection methods, imaging protocols, and mechanical testing procedure created by the Bone and Joint Research Lab at the University of Ottawa [47]. Emphasis will be on the Mechanical testing section, as this work was conducted by the author of this thesis.

## 4.2 Surgical Procedures

Two surgeries were performed, during which the rabbits received an intramuscular injection of ketamine (25 ng/kg), midazolam (2 mg/kg), and glycopyrrolate (0.1 mg/kg) prior to being put under general anesthesia using a face-mask that provided isoflurane (2-3%) and oxygen (1-2 L/min) [47]. The contralateral legs served as controls and remained untouched during surgery. All surgeries were performed by lab technicians (Ying Nie and Marie-Eve Methot) with veterinary supervision.

The following sections describe the surgical procedures conducted to create both Achilles tendon models.

### 4.2.1 Model of Ischemia Induced Degeneration (Groups 1 and 2)

The first step was to block intra-tendinous vascularization, which is the blood supplied through the vessels inside of the tendon. A longitudinal posterolateral skin incision was made to allow for the opening of the crural fascia and Achilles paratenon. The tendon sheath was then opened and two sutures were tied around the tendon at 10 mm and 35 mm proximal to the calcaneal insertion to block intra-tendinous vascularization in this region.

The next procedure was to block the extra-tendinous vascularization, which is the blood supplied through diffusion from the paratenon. A millipore membrane, permeable to water ions but impermeable to cells, was wrapped around the tendon beneath the paratenon and three sutures were tied around the membrane securing it in place. Please see Figure 12(a) on page 40 for a detailed illustration of the procedure.

Finally, a continuous skin suture was performed leaving the paratenon and fasciae to spontaneously cover the surgical site without sutures.

Post-operative treatment consisted of:

- unrestricted activity in group housing
- food and water ad libitum
- administration of buprenorphine (100 mg/kg) administered subcutaneously, at regulated time intervals, up until postoperative day three.

A fentanyl transdermal patch (Duragesic 25, Janssen-Ortho Inc., Markham, ON, Canada) was also applied to shaven skin one day prior to surgery and removed four days post-operatively, to aid in pain relief.

At the time of the second surgery, four rabbits were prematurely euthanized due to necrosis and/or rupture of the tendon and were not used in this study. The contralaterals to the prematurely euthanized rabbits were considered invalid. Even though the contralaterals were not touched, the rabbits behavior during injury affects the strength of the tendon rendering them invalid as controls for this study.

The second surgery was performed eight weeks after the first surgery. A longitudinal posterolateral skin incision was made to allow for the re-opening of the crural fascia and Achilles paratenon. The tied sutures and millipore membrane used for strangulation were then removed. Six experimental tendons, from Groups 1 and 2, remained. Three of these experimental tendons were allowed to heal (Group 1 - Strangulated) and the other three underwent a full thickness partial tendon injury (Group 2 - Strangulated & Punched), as described in the next section.

#### **4.2.2 Model of Full-Thickness Partial Tendon Injury in Tendons with Ischemia Induced Degeneration (Group 2)**

A custom Achilles tendon punch instrument was used to create a partial tendon injury in Group 2 tendons (designed by Philippe Poitras at the Bone and Joint Lab., shown in Figure 13 on page 41). The punch removes approx. 50 % of the tendon fibers by creating a full thickness oval defect 3 mm (width) by 7 mm (length) (See Figure 14, page 42), at a position 20 mm proximal to the insertion, as seen in Figure 12(b). The outer edges of the tendon were left intact, preserving the continuity of the tendon on both sides of the defect. This defect location corresponds to the site of most common injury in human Achilles tendons.

Finally, a continuous skin suture was performed leaving the paratenon and fasciae to spontaneously cover the surgical site without sutures.

Post-operative treatment followed the same protocol as with the first surgery.

### **4.3 Collection and Storage of Specimens**

The specimens were collected at either 2 or 4 weeks after the second surgery. The animals were euthanized using an overdose of pentobarbital (100 mg/kg, i.v.). One degenerated tendon (Model 1) and one punched degenerated tendon (Model 2) were harvested at two weeks, while the remaining four tendons were harvested at 4 weeks. The bilateral calcaneus-Achilles tendon-gastrocnemius-soleus muscle complex were resected en bloc after dissection. All specimens were wrapped in saline soaked gauze and stored at -29°C until testing. Specimens were thawed to room temperature for

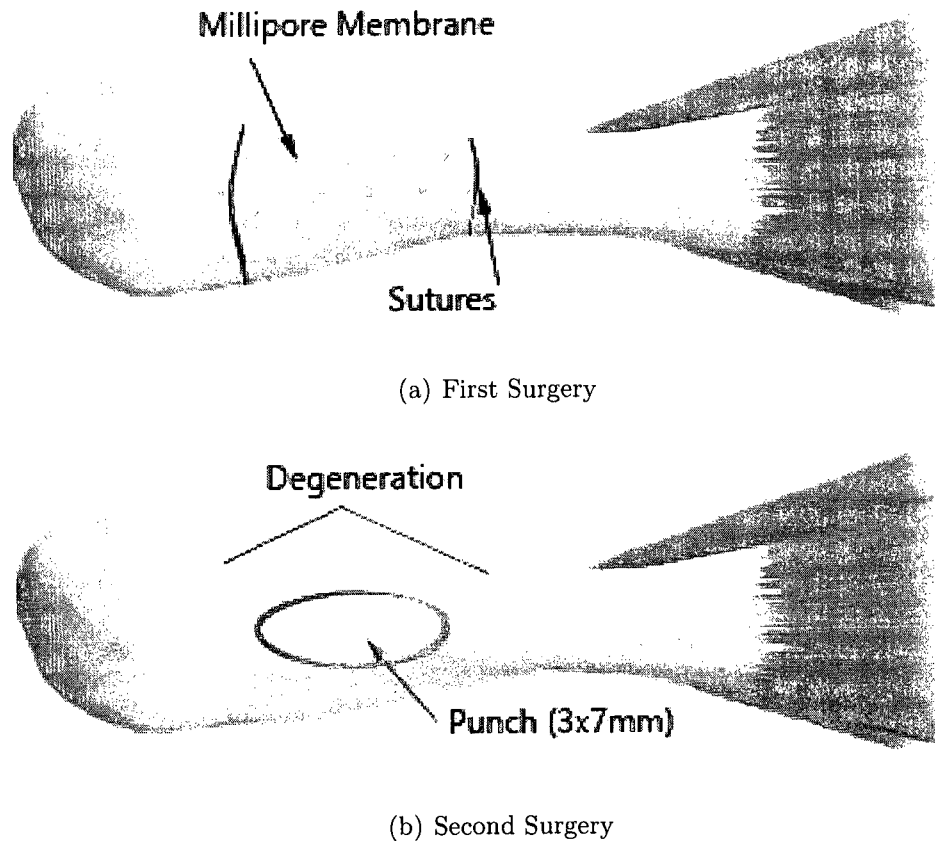
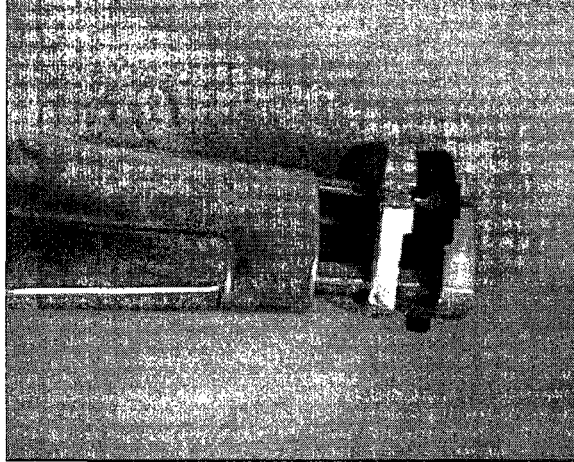
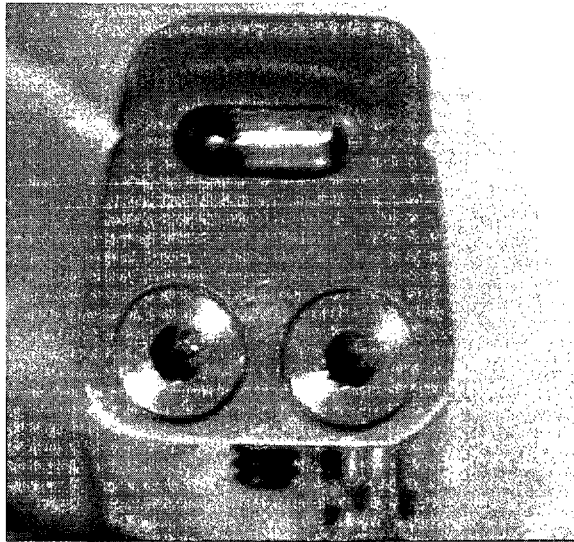


**Figure 12:** Surgical Procedures. The first surgery (a) consists of wrapping two sutures around the tendon (beneath the tendon sheath), at 10 and 35 mm from calcaneal insertion. A Millipore membrane is then wrapped around the tendon and three sutures are tied around the tendon and membrane, to holding the membrane in place. The second surgery (b) removes the membrane and sutures and in half the tendons, punches a full-thickness hole through the center at 20 mm (from calcaneal insertion). Illustrated by Jeffrey Bruton for use in this thesis.



(a) Side View



(b) Front View

**Figure 13:** Tendon punch. This custom designed punch (by Philippe Poitras at the Bone & Joint Lab) is used to remove a full thickness area of tissue (7mm by 3mm) corresponding to a loss of 50% of the rabbit Achilles tendon fibers. Punching of the tendon simulates human Achilles tendon injury [47].



**Figure 14:** Acute punch injury in a rabbit Achilles tendon resulting from the custom punch in Figure 13 [47].

clinical imaging.

## 4.4 Imaging

Three types of imaging were used for Model analysis. Diagnostic ultrasound images were used to measure the dimension of the tendons at 5 mm intervals along the length of the tendon, between 5 mm and 35 mm from the calcaneal insertion. Magnetic resonance imaging was used to measure the signal intensities and dimensions of the tendons at 20 mm from the calcaneal insertion. X-rays were used to measure the bone mineral density of the calcaneal bone attached to each tendon. The Protocols are described in detail below.

#### 4.4.1 Diagnostic Ultrasound Imaging (US)

An HDI 5000 (Philips) ultrasounds (US) machine was used by an experienced sonographer (Jane St. Germain, US technologist) to capture the US images of the Achilles tendon specimens. The maximal transverse and anteroposterior measurements of the tendons were taken at 5 mm intervals along the gauge length (5 mm - 35 mm proximal to the calcaneal insertion), using a CL10-5 transducer.

#### 4.4.2 Magnetic Resonance Imaging (MRI)

All MR images were obtained by Francine Mccullagh, MRI technologist, and read by Dr. Kawan Rakhra. Groups of 6 thawed tendons were placed in a saline-filled, watertight, and MRI compatible tendon box (see Figure 15, custom designed by Nanthan Ramachandran at the Bone and Joint Lab.). This box allows for proper alignment of the tendons during imaging. At 2 mm slice thickness, three sequences were recorded using a Siemens Symphony 1.5 T MRI unit and its extremity coil: axial T1 spin echo (TR 400, TE 14, NEX 2, FOV 130 mm, matrix 576 X 576), axial dual echo (TSE) (TR 4680, TE 14/84, NEX 2, FOV 130 mm, matrix 576 X 576), and sagittal T1 TSE (TR 2720, TE 20, NEX 3, FOV 130 mm, matrix 512 X 440) [47].

The dimensions and optical densities at the site of injury were then measured. The anteroposterior and transverse dimensions of the tendon were measured at 20 mm proximal to insertion (site of injury). The site of injury was then defined as an oval shaped region-of-interest in the axial plane and the mean optical density for each of the T1, proton density, and T2-weighted MRI sequence was measured.

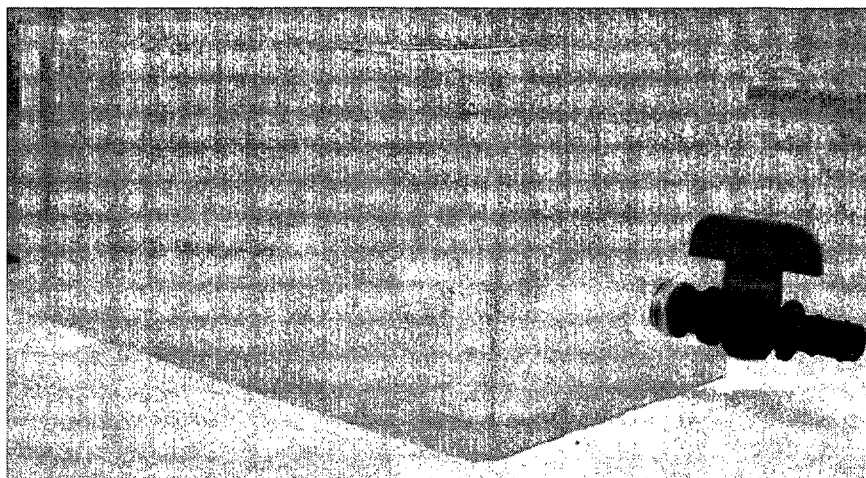


**Figure 15:** Tendon Box. Specially designed saline-filled, water-tight, and MRI and US compatible tendon box that holds and properly aligns six (6) tendons for diagnostic imaging [47]. Designed by Nanthan Ramachandran at the Bone and Joint Lab.

### Measuring the Cross-Sectional Areas

The cross-sectional area of each tendon at 20 mm from the calcaneal insertion was calculated by the author of this thesis. Exported transverse MR images and software (ImageJ version 1.42, by Wayne Rasband, National Institute of Mental Health, Bethesda, Maryland, USA) were used to measure the cross-sectional area of the user-outlined regions. The area of each tendon was calculated using two different methods and the mean of the two values was taken to be the cross-sectional area of the tendon. The first method involved increasing the contrast of the image, magnifying the image, and manually outlining the image with the cursor. The second method involved increasing the contrast and then selecting the tendon area by selecting the threshold of the shaded area. By selecting the threshold, a coloured mask covered the darkened area of the tendon so that it could be selected and the area measured. It should be noted that the two areas obtained from the two methods were very close in value. These areas were later used to calculate the peak mean stress in the tendons.

### 4.4.3 Calcaneal Bone Mineral Density (BMD)

All BMD measurements were taken by Philippe St. Laurent, technologist. The tendon specimens were submerged in a raw rice filled container during imaging. The rice simulates the natural soft tissue environment of the specimen. A Dual Energy X-ray Absorptiometer (DPX-alpha, Lunar Corp.) and software (SmartScan version 4.7e, Lunar Corp.) enabling small bone imaging, measured the bone mineral density of the whole calcaneus. The x-ray beam was directed from the dorsum to the plantar aspect of the calcaneus.

## 4.5 Mechanical Testing

Mechanical testing consisted of applying a tensile load to the tendon until rupture. At this point the peak load to failure was recorded and used to indicate the strength of the Achilles tendon. A dual cryogenic fixation apparatus (see Figure 19, page 51, designed by Nanthan Ramachandran at the Bone and Joint Lab.) was used to securely hold both proximal and distal ends of the tendon while the loading frame (MTS Sintech 1G, MTS Systems Corporation, Eden Prairie, MN, USA) applied the tensile load. All mechanical tests were conducted by the author of this thesis. The materials and methods used for mechanical testing of the tendons are listed in this section.

### 4.5.1 Materials & Equipment

- Tendon Specimens (Bilateral calcaneus-Achilles tendon-gastrocnemius-soleus muscle complexes (Figure 16, page 47))
- Sutures or Needle and thread

- Blue India Dye
- 50 mL of 0.1% Saline Solution
- 1.5 L of Liquid Nitrogen
- Duo-cryogenic fixation assembly (Figure 19, page 51)

#### **4.5.2 Methods of Preparing and Mechanically Testing the Tendon Specimens**

After Imaging, the tendon specimens (bilateral calcaneal-Achilles tendon-gastrocnemius-soleus muscle complexes) were prepared and mechanically tested.

They were:

- thawed and prepared for mounting
- mounted in the duo-cryogenic fixation apparatus
- thermally controlled and monitored
- tested for peak load to failure

Finally, the peak mean stress of each tendon was calculated. These steps are described in the following sections.

##### **Specimen preparation**

The preparation for mounting included thawing and sizing the specimens. The frozen specimens were thawed in water, at room temperature (approx. 30 minutes) until completely thawed. To prepare the specimens for testing, the gastrocnemius-soleus muscle was shaved down, removing unnecessary muscle tissue so that the muscle

end of the tendon could easily fit between the holding rods in the core ice chamber. The end of the muscle was also trimmed leaving about 3 cm of muscle attached to the tendon, eliminating excess muscle and maintaining enough tissue to be frozen in the fixation. In the case where the calcaneal bone was too thick to pass through the holding rods in the ice chamber, portions of the bone were removed.

Sutures were then used to indicate the gauge length and provide a guide. Three sutures were wrapped around the tendon at the: site of calcaneal insertion, beginning of the gauge length, and end of the gauge length (Figure 16). A fourth suture was wrapped and sewn at about 50 mm proximal to insertion with approximately 127 mm of excess suture material left. This last suture material was used as a guide to thread the muscle end of the specimen through the holding rods in the ice chamber.

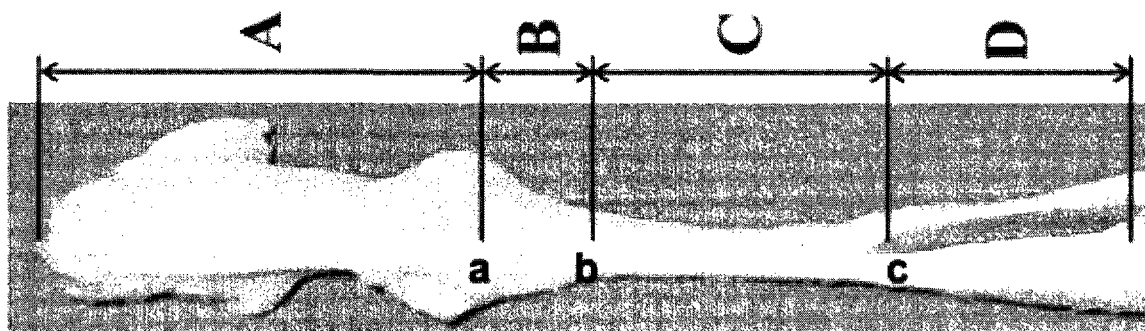


**Figure 16:** The Rabbit Achilles Tendon Specimen. *Length A* represents the calcaneus bone area that is frozen along with *length B* in the TOP ice container. *Point a* is the insertion point. *Point b* is 10 mm from the insertion point and marks the beginning of the gauge length and ice limit. *Point c* is 25 mm from *point b* and marks the end of the the gauge length and second ice limit. *Length D* represents the proximal area frozen in the BOTTOM fixation. At the end of *length D*, a fourth suture is attached to allow for threading through the BOTTOM ice chamber [31].

Finally, blue india dye was painted on the anterior surface of the specimen and allowed to dry before mounting so as to maintain proper orientation of the tendon

after rupture.

### Specimen fixation

The tendon defect was centered between two fixations with a gauge length of 25 mm, spanning 10 mm to 35 mm proximal to insertion. The calcaneal portion of the specimen was fixed by the top fixation and mounted to the loading frame before the muscle portion of the tendon could be fixed by the bottom fixation. The suture attached to the muscle portion of the tendon (in length D) was used to thread the tendon through the holding rods in the bottom fixation (Figure 17), while the top fixation was lowered.

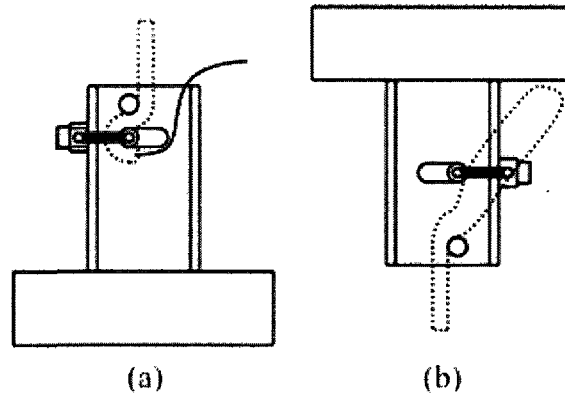


**Figure 17:** Tendon Specimen fixed in both the Bottom (a) and Top (b) cryogenic fixations [31].

The full mechanical testing protocol, including preparation procedures, are included in Appendix A.

## Thermal control and monitoring

Thermal control was obtained using a heater and insulators. A heater was used to prevent freezing of the gauge length of the tendon while the bottom fixation was frozen with the liquid nitrogen. Petroleum jelly was applied to the tendon to prevent dehydration from the heater. Insulators covering the ice surfaces were used to prevent melting of the ice. The heater and insulators allowed for a sharp temperature gradient, as seen in Figure 18, where the defect area was at body temperature ( $37^{\circ}\text{C}$ ), and the ice temperatures were maintained at approximately  $-20^{\circ}\text{C}$ .

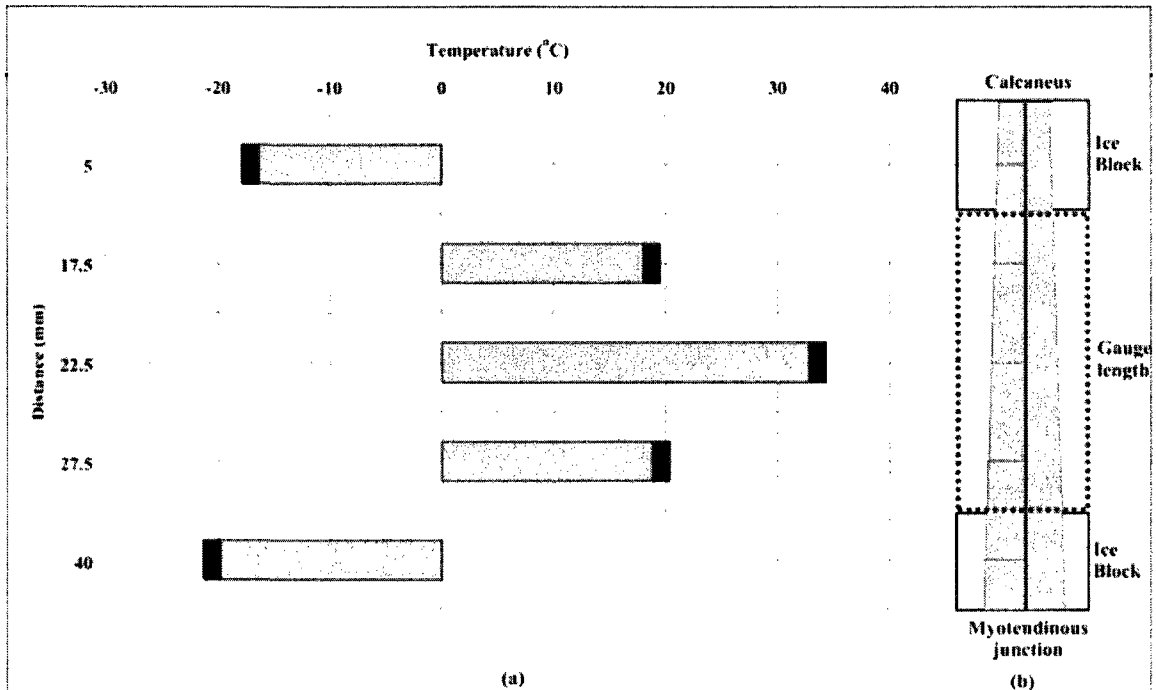


**Figure 18:** Representative thermal profile of a rabbit Achilles tendon using the dual cryogenic fixation system seen in Figure 19. The sharp temperature gradient between the fixed ends and the midsection of the tendon ensures that the ice rigidly fixes the tendon while the midsection of the tendon is at body temperature. The dark bars represent the temperatures during mechanical testing [47].

The thermocouples embedded in both cryofixations allowed for continuous monitoring of the ice temperatures. Monitoring was conducted using two K-type thermocouples attached to a thermometer (MONARCH 309), embedded 10 mm

below the ice surface in each ice chamber. Test links SE 309 software was used to collect and graph the data. Mechanical testing was conducted when the thermocouples indicated ice temperatures of approximately  $-20^{\circ}\text{C}$ .

### **Mechanical testing**

The peak load to failure was determined by applying a tensile load at a displacement rate of 10 mm/s until a 50% decrease in load was detected. The rate of displacement was selected based on high-velocity clinical conditions that lead to Achilles tendon rupture. All tendons were preconditioned at a rate of 18 N/s to a peak load of 30 N for 10 cycles, before testing for failure.

Data on load and crosshead displacement was collected at 100 Hz, and a load-deformation curve, like the one in Figure 20, was generated using the mechanical test software (TestWorks 4, MTS Systems Corporation, Eden Prairie, MN, USA).

### **Calculating the mean stress at peak load**

The mean stress in each tendon at peak load to failure was calculated using the peak load at failure, and dividing it by the corresponding cross-sectional area (at 20 mm proximal to the calcaneal insertion) obtained from the MR images. This stress is not the true stress as the area used is not the deformed area. This deformed area may be significantly different from the unloaded area.

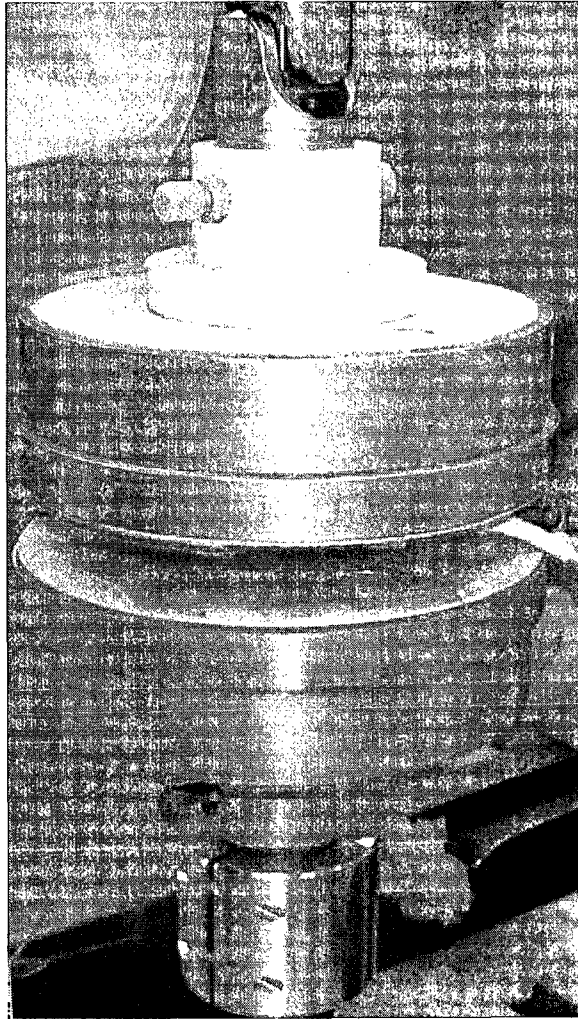


**Figure 19:** Cryogenic Fixation System. The top and bottom cryofixations rigidly grasp both ends of the specimen at 5 mm and 35 mm proximal to the calcaneal insertion allowing for a 25 mm long gage length. The cryogenic fixations are attached to the loading frame (Sintech 1/G, MTS Systems Corp, Eden Prairie, MN) so that testing loads can be applied to the specimen in isolation [47]. Designed by Nanthan Ramachandran at the Bone and Joint Research lab.

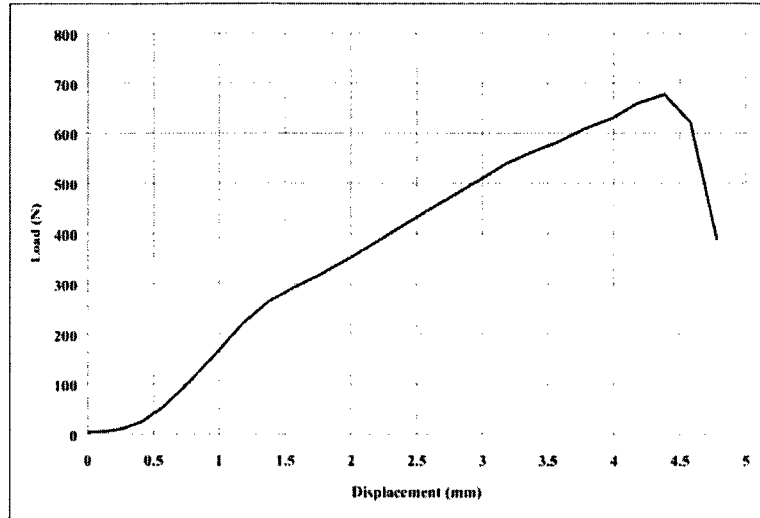


**Figure 20:** Sample of a typical Load vs. Displacement curve during mechanical testing of rabbit Achilles tendons. This curve simulates a high-load clinical condition leading to full rupture of the achilles tendon [47].

### 4.5.3 Data Analysis

Percent differences were used to compare the data. This study was conducted as a pilot study for further research into a new Achilles tendon models and therefore the sample sizes were small. Because of the small sample sizes, no statistically significant analysis could be performed. The results obtained using the images and mechanical testing methods were compiled, by the author of this thesis, according to their experimental group and healing time. The mean values were then compared as percent differences. All data points were also plotted and any apparent correlation or trend documented in the following results chapter.

## Chapter 5

# Experimental Results

This chapter contains a summary of the imaging (MRI, US, and BMD) and mechanical (Peak Load to Failure and Stress) results obtained using the experimental methods described in the previous chapter. Full results are presented in Appendix C.

### 5.1 Imaging Results

Three types of images were taken and used to analyze the tendon groups. The following section contains the results of the Diagnostic Ultrasound Images (US), Magnetic Resonance Images (MRI), and Bone Mineral Density Measurements (BMD).

#### 5.1.1 Diagnostic Ultrasound (US) Imaging

Ultrasound imaging was used to compare the cross-sectional size of the tendons at 2 week and 4 week healing times. The anterioposterior (AP) and transverse (TR) measurements from the ultrasound images of all of the tendons were taken by a certified technologist and read by a radiologist, blinded to the identity of the

tendons. Measurements were made at 5 mm intervals, between 5 mm and 35 mm from the calcaneal insertion, for all tendons (Table 2).

**Table 2:** Mean Ultrasound Anteroposterior and Transverse Tendon Measurements (mm) (T = healing time in weeks, and n = sample size)

Group*	T	n	5mm		10mm		15mm		20mm		25mm		30mm		35mm	
			AP	TR	AP	TR	AP	TR	AP	TR	AP	TR	AP	TR	AP	TR
1	2	1	5.3	9.0	4.1	10.9	4.5	5.5	3.7	4.9	2.8	6.8	3.0	8.3	3.5	10.0
1	4	2	4.8	6.8	4.8	7.0	4.2	5.9	2.9	4.6	2.8	4.6	2.7	5.5	2.7	7.6
2	2	1	5.5	6.5	5.1	8.0	4.3	7.4	4.9	6.9	5.1	7.1	5.6	9.9	6.6	16.5
2	4	2	5.6	9.4	5.1	9.0	3.8	7.2	3.6	6.5	3.6	7.3	3.2	7.6	3.2	8.3
3	-	6	5.9	6.4	3.9	5.9	3.4	5.4	3.0	5.1	3.2	6.4	3.5	7.6	3.4	9.2

\*1- Strangulated, 2 - Strangulated & Punched, 3 - Contralateral

The focus of the data in this table are the dimensions at the site of injury (20 mm from insertion). This is the region of inflammation. At this site, Group 1 (Strangulated) showed little change in AP size regardless of healing time. The only large change in mean AP and TR is seen in Group 2 (Strangulated & Punched). In these tendons, the mean AP and TR, at 2 weeks healing time, are respectively 40% and 27% larger than the contralateral tendons. The mean AP normalized by 4 weeks healing time, but the mean TR remained enlarged

### 5.1.2 Magnetic Resonance Imaging (MRI) Results

Magnetic resonance images (MRIs) were used to calculate the cross-sectional areas, and T1, PD (Proton Density), and T2 optical densities (OD) (See page 10 for more details), at the site of injury (20 mm proximal to the calcaneal insertion). The mean values for each experimental group are in Table 3.

The mean cross-sectional areas of both experimental Groups 1 and 2 were

larger compared to the contralateral group (3), at both healing times. Group 1 (Strangulated) maintained a 30% increase in cross-sectional area 2 and 4 weeks after surgery. Group 2 (Strangulated & Punched) had the largest change in cross-sectional area with an 87% increase in size at 2 weeks, and 50% increase at 4 weeks.

**Table 3:** Mean Cross-sectional Areas and Optical Densities of the Experimental Groups Obtained Using Magnetic Resonance Imaging (MRI)

Group	Healing Time	Sample Size	Area (mm <sup>2</sup> )	Sequence		
				T1 OD	PD OD	T2 OD
1	2 Weeks	1	17.5	107	163	154
1	4 Weeks	2	18.4	118	183	155
2	2 Weeks	1	92.1	460	780	215
2	4 Weeks	2	24.3	181	373	200
3	-	6	12.0	156	199	192

\*1- Strangulated, 2 - Strangulated & Punched, 3 - Contralateral

The T1 ODs were lower in Group 1 and higher in Group 2, than the contralaterals. Group 1 maintained a 30% lower OD than the contralaterals throughout the 2 and 4 week healing times. Group 2 started with a mean T1 Value 66% higher than the contralaterals and returned to contralateral values by 4 weeks.

The PD ODs for Group 1 decreased while the values for Group 2 increased. Group 1 barely deviated from the contralateral values with a 22% decrease in OD at 2 weeks and returned to contralateral values by 4 weeks. The ODs for Group 2 however, were 75% higher at 2 weeks and 47% higher at 4 weeks, than the contralaterals.

The T2 ODs for Group 1 decreased and unusual values for Group 2 were observed. Group 1 remained approximately 25% lower than the contralateral values at both 2

and 4 week healing times. Group 2 did not deviate from the contralateral values at 2 weeks, but increased by approximately 30% at 4 weeks. The increase at 4 weeks was unexpected and may be an outlier result.

### 5.1.3 Bone Mineral Density (BMD) Results

A dual energy X-ray absorptiometer was used to measure the calcaneal bone mineral densities. The mean values for each experimental group are listed in Table 4. No change in BMD was observed between Groups (1, 2, and 3).

**Table 4:** Mean Bone Mineral Densities (BMD) of All Experimental Tendon Groups

Group	Healing Time	Sample Size	BMD (% of Contralateral) (g/cm <sup>2</sup> )
1	2 Weeks	1	0.353 (92%)
1	4 Weeks	2	0.375 (98%)
2	2 Weeks	1	0.347 (91%)
2	4 Weeks	2	0.350 (91%)
3	-	6	0.383 (100%)

\*1- Strangulated, 2 - Strangulated & Punched, 3 - Contralateral

## 5.2 Mechanical Testing Results

All tendons were mechanically tested for peak load to failure and the peak mean stress in the tendons were calculated. The results for four tendons were not valid due to technical difficulties during mechanical testing. Failure at the site of fixation deemed the results invalid. Stress was calculated using the peak load to failure values and the cross-sectional areas (from MRI) of each tendon.

Table 5 indicates no difference in tendon strength between experimental groups 1 (Strangulated) and 2 (Strangulated & Punched), but both were weaker than the contralaterals at 2 weeks. The mean peak load to failure results also showed complete recovery of strength by 4 weeks when compared to the contralaterals. A 44% difference in average peak load to failure between the 2 week and 4 week healing times, however, was observed. The largest decrease in strength (30%) was in Group 1 at 2 weeks healing time.

**Table 5:** Mean Peak Load to Failure and Stress of All Experimental Tendon Groups

Group	Healing Time	Sample Size	Failure Load (N) (% of Contralateral)	Stress (MPa) (% of Contralateral)
1	2 Weeks	1	543 (67%)	31.1 (49%)
1	4 Weeks	2	802 (99%)	43.1 (67%)
2	2 Weeks	1	690 (85%)	7.5 (12%)
2	4 Weeks	1	1067 (131%)	35.4 (55%)
3	-	4	810 (100%)	63.9 (100%)

\*1- Strangulated, 2 - Strangulated & Punched, 3 - Contralateral

Even though there was no change in peak load observed at 4 weeks, there was a large change in stress. The mean stress values were substantially lower in all tendon experimental groups 1 and 2 tendons at 2 and 4 weeks. Group 1 had mean stress values 49% and 67% of the contralateral values at 2 and 4 weeks, respectively. Group 2 had an even larger decrease in mean stress with only 12% and 55% of the contralateral values at 2 and 4 week healing times, respectively. In both cases, the stresses were still substantially lower than the contralateral at 4 weeks, with Group 2 tendons showing the largest change.

### 5.3 Possible Correlation of Imaging Outcome Measures with Mechanical Properties

The results were plotted and compared for visual trends because insufficient data was collected to calculate any statistically significant correlation. Visible trends observed between Group 2 variables suggest that an increase in T1 signal intensity correlates with a decrease in peak load to failure (see Figure 21) and a decrease in stress (see Figure 22). A decrease in stress also correlates with an increase in PD signal intensity (see Figure 23). Finally, an increase in BMD correlates with an increase in stress (See Figure 24). No visible trend was observed between Group 1 and contralateral variables.

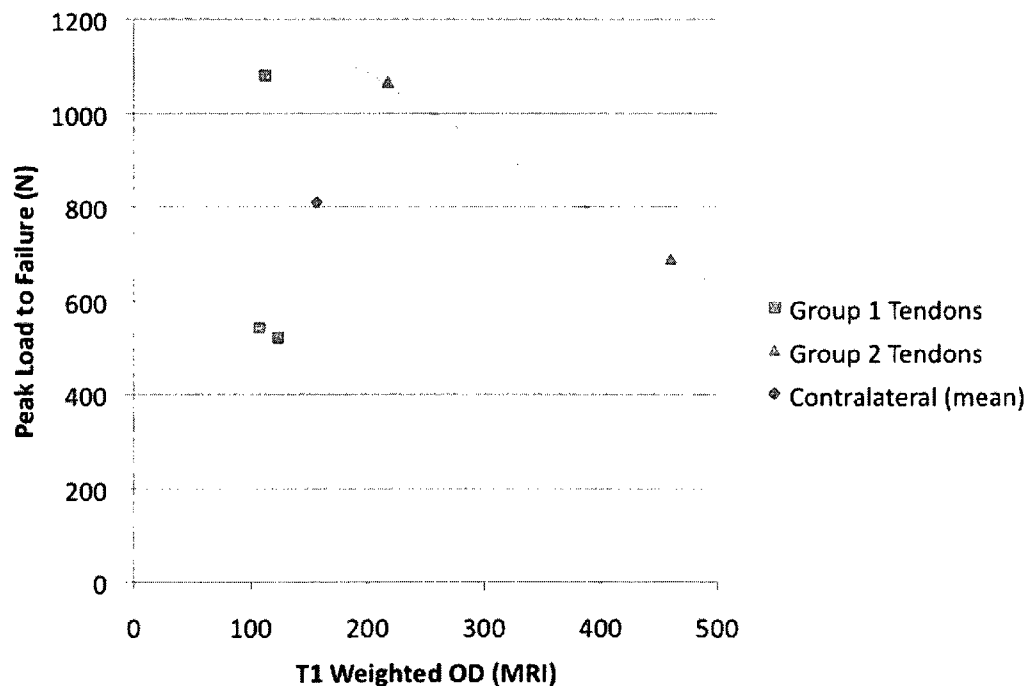


Figure 21: Tendon Peak Load vs. T1 Weighted Optical Density

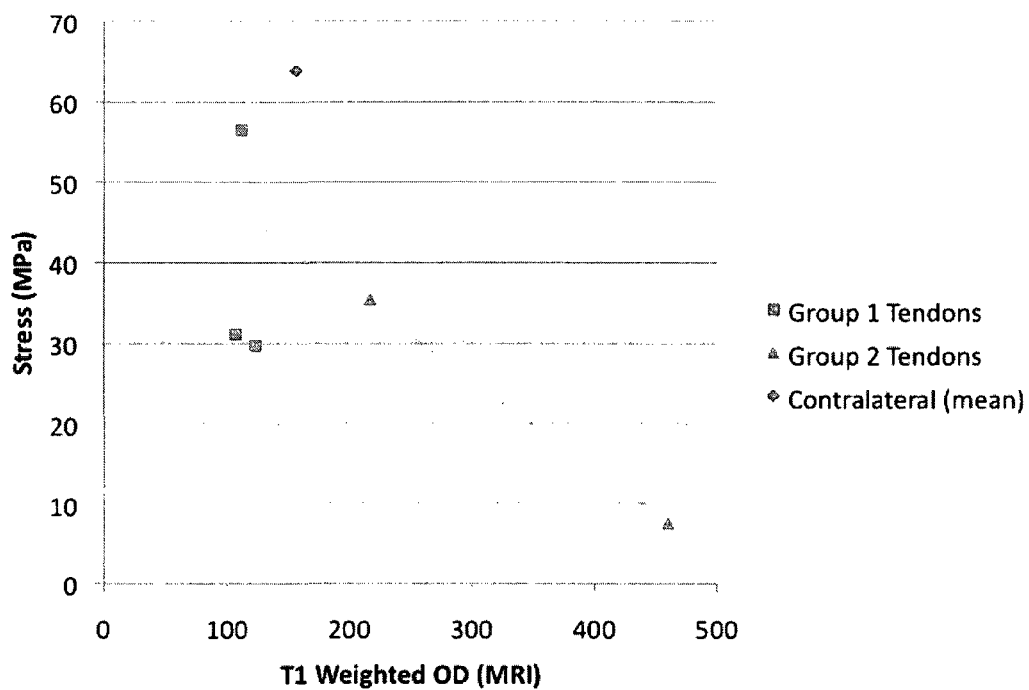


Figure 22: Mean Tendon Stress vs. T1 weighted Optical Density

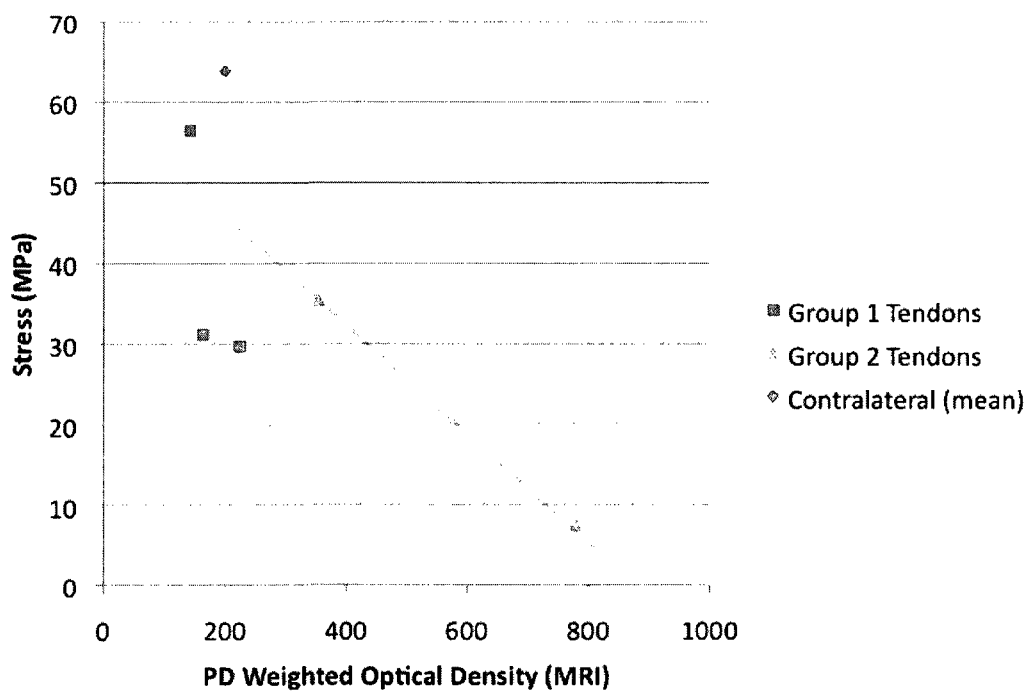


Figure 23: Mean Tendon Stress vs. Proton Density Optical Density

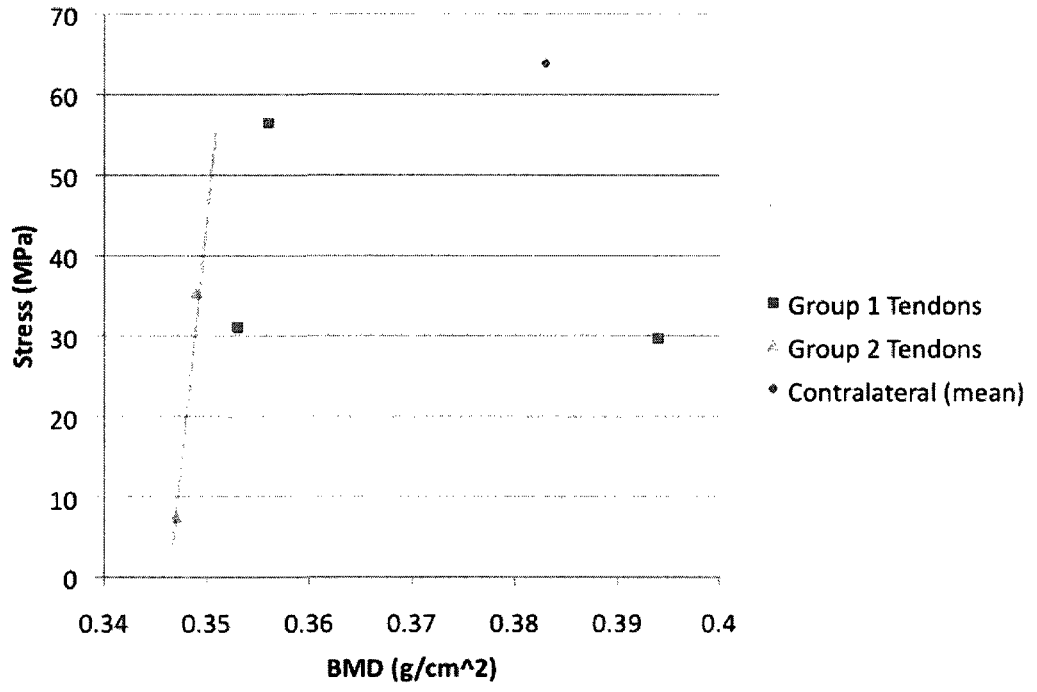


Figure 24: Mean Tendon Stress vs. Calcaneal Bone Mineral Density

## Chapter 6

# Discussion of Results

This chapter includes a detailed interpretation of the results of this study, analyzes the main hypothesis of the study, and discusses new hypotheses that have arisen from the work in this thesis.

To analyse the hypothesis, that tendons with pre-existing degeneration are slower to recover their mechanical properties than healthy tendons with the same injury, Model 2 (Degenerated & Punched) is first compared to Model 1 (Degenerated) and then compared to the healthy model created in the previous study, by the Bone and Joint Laboratory. Model 1 (Degenerated) acts as an experimental control for Model 2 (Degeneration & Punch) and, when compared to contralateral values, allows us to see what effect ischemia induced degeneration has on rabbit Achilles tendons and their mechanical properties. Once this effect is known, the hypothesis is tested by comparing Model 2 to the healthy model.

Possible correlations between imaging and mechanical values are then investigated to determine if a correlation exists that may improve the clinical management of Achilles tendons after injury or repair. The final portion of this discussion compares the rabbit Achilles tendon models to human Achilles tendons.

## 6.1 Model 1 - Ischemia Induced Degeneration

The purpose of Model 1 was to test the effects of ischemia induced degeneration on the mechanical strength of rabbit Achilles tendons. The model was also used as an experimental control for Model 2 (Strangulated & Punched) tendons. The tendons in Model 1 were strangulated, blocking both the extra- and intra- tendinous vascularization, to simulate degeneration. Intratendinous vascularization was restricted by wrapping two sutures around the tendon, at 5 mm and 35 mm proximal to the calcaneal insertion, beneath the tendon sheath. Extratendinous vascularization was blocked using a semi-permeable Millipore membrane and securing it around the tendon, beneath the tendon sheath. The tendons were strangulated for a period of eight weeks. The strangulating material was then removed and the tendons allowed to heal for either two or four weeks after surgery. The tendons were then imaged and mechanically tested.

Imaging results (US and MRI) showed an expected increase in cross-sectional area. Increases in tendon size have been correlated with tendinopathy, tendon injury, and healing. The Model 1 tendons were 30% larger at both two and four weeks after surgery. Any changes in cross-sectional area beyond four weeks were not determined in this study. These results confirm that some form of tendinopathy was created, however, it is unclear if it is degeneration. Additional studies with samples taken at more frequent healing times (ex.  $t = 1,2,3,4,5,6\dots$  weeks) are necessary for further analysis.

The MRI optical density (OD) results showed an unexpected decrease (lower than those of the contralateral) in all three types: T1 weighted, Proton Density (PD), and

T2 weighted. T1 and T2 values did not change from two to four weeks, however, PD values returned to contralateral levels by four weeks. Higher T2 weighted optical densities were expected as are observed in human tendons with degeneration. This increase in T2 OD is a result of edema and increased water content in tendons healing from tendinopathy. Healthy tendons normally give low T2 OD readings. To determine what may have caused a further decrease in T2 OD histology is required.

The peak load to failure recovered with a significant decrease in peak mean stress. The mechanical strength (measured as peak tensile load to failure) of the Model 1 tendons recovered 80% of their strength by two weeks, with full recovery by four weeks. The mean stress, however, dropped to 49% at two weeks and had only recovered 67% by four weeks. This decrease in stress is attributed to an increase in cross-sectional areas since stress is a function of force over cross-sectional area.

The unexpected recovery of strength by four weeks, suggests that:

- Degenerated tendons recover their mechanical strength faster than expected,
- Our degeneration model caused insufficient damage to simulate human degeneration, or
- Mean stress levels are a more accurate indicator of tendon health.

Additional work that involves investigating degenerated tendons immediately after surgery (i.e. no healing time) is necessary to validate model 1.

A histological analysis is required to determine the load bearing mechanisms of the material associated with the increased cross-sectional area, observed during the healing process. In this study, an evenly distributed load was assumed for mean

stress calculations.

The data from the imaging and mechanical testing results, set the base for the second model.

## **6.2 Model 2 - Ischemia Induced Degeneration and Acute Injury**

This model was created in response to a previous study conducted by the Bone and Joint Laboratory at the University of Ottawa, where they hypothesized that tendons with pre-existing degeneration are slower to recover their mechanical properties than healthy tendons with the same injury. Imaging and mechanical testing results were obtained, for each specimen, for comparison between studies.

At the time of the second surgery, when the strangulating material was removed, half of the tendons received centered full thickness partial tendon tears (by a custom punch that removes 50% of the tendon tissue at mid-substance). This disruption of the collagen fibers was designed to simulate acute injury, while leaving the outer edges of the tendon intact to prevent propagation of the tear. After injury, the tendons were allowed to heal for either two or four weeks, as the tendons in Model 1 did.

Model 2 results (MRI, US) showed cross-sectional areas larger (by 60%) than those of the Model 1 tendons. This was expected as an increase in size indicates that the tendons are still in an early stage of the healing process. Tendon size is largest

at the initial stages of healing.

All Model 2 optical densities (OD) were larger than the Model 1 and contralateral ODs. The T1 weighted OD was the only density to recover by four weeks. The largest increase in OD was observed with PD images: a 75% increase at two weeks and 47% increase at four weeks. Considering that the base ODs (from Model 1) were below those of the contralaterals, there appears to be a significant increase in ODs as a result of injury.

No change in BMD between Models 1 and 2, and the Contralaterals was observed.

Contradictory to expectation with human injuries, the mechanical results showed complete recovery of the mechanical strength (peak tensile load to failure) by four weeks, despite the added strangulation. These results are inconsistent with human clinical expectations, where healing is believed to take as long as twenty-six weeks.

Both Models 1 and 2 indicate that tendons recover mechanical strength early after injury or surgical repair by increasing the cross-sectional area and thus reducing the stress. As previously seen with Model 1, the mean stress dropped significantly with increased area. As little as 12% of the stress was recovered at two weeks, and 55% at four weeks.

Testing the hypothesis, that tendons with pre-existing degeneration are slower to recover their mechanical properties than healthy tendons with the same injury, requires the comparison of Model 2 (Strangulated & Punched) to the model of acute injury in healthy tendons from the previous study.

### 6.3 Comparison of Study Results to Test the Hypothesis of this Study

Previous work by the Bone and Joint Laboratory at the University of Ottawa [1] characterized the mechanical properties of rabbit Achilles tendons at various healing times after surgically creating a large central defect (punch) to healthy tendons. They also assessed the ability of imaging modalities (US, MRI, BMD) to predict the mechanical properties of rabbit Achilles tendons after injury. For the purposes of clarity, the tendon model in this previous study will be referred to as the "healthy" model and Model 2 from the thesis study will be referred to as the "degenerated" model.

The healthy model tendons recovered their mechanical strength by four weeks [1], while the imaging results (cross-sectional area, ODs) remained abnormal. A decrease in mean stress, however, was observed with the increase of the cross-sectional area. These results led to the belief that adding degeneration to our model, before injury, would reduce the recovery rate. This idea is based on the fact that human tendons are thought to suffer from some form of degeneration prior to injury or rupture, and that human tendons take longer to recover their mechanical strength.

To test this hypothesis, the data from the healthy model are compared to the degenerated model. Due to the small sample sizes in these studies comparisons are purely prospective.

The results suggest that the degenerated tendons take longer to normalize their size and ODs and therefore they take longer to heal than the healthy tendons. The degenerated tendons were 78% and 22% larger than the healthy tendons, at 2

and 4 weeks respectively. All T1 weighted, PD, and T2 weighted optical densities were also approximately 40% higher in the degenerated tendons versus the healthy tendons, at 2 weeks. At 4 weeks, the only increase in OD was seen in T2 OD with a 29% higher value for the degenerated tendons. The complete set of results from the previous study on healthy tendons with acute injury are presented in Appendix D.

The hypothesis that tendons with degeneration are slower to recover their mechanical properties than healthy tendons is disputed according to this data. Despite evidence of slower recovery rate, the mechanical strengths of both tendon models do not differ. Therefore, the mechanical strength of the tendons recovers at the same rate, despite degeneration.

Stress reduction in the early stages of healing and the significantly lower stress values for degenerated tendons suggest that stress or cross-sectional area is a more accurate representation of healing.

In summary, the degenerated model was slower to recover all properties, except peak load to failure, than the healthy model. These results have led to the hypothesis (A): tendons recover their mechanical strength early after injury or surgical repair, and the recovery is accomplished by increasing the cross-sectional area, thus reducing stress. This hypothesis was first developed in the previous study [1].

From the data collected in both studies, correlations between variables can be analyzed in hopes of aiding in the prediction of the mechanical properties of tendons using imaging modalities (MRI, US, BMD).

## 6.4 Correlation between Variables

In both rabbit Achilles tendon studies (healthy [1] and degenerated), correlations between variables were discovered. The healthy model study had large enough sample sizes for statistical analysis of correlation, and found that:

1. An increase in T1 OD correlates with a decrease in peak load to failure
2. An increase in T1 OD correlates with a decrease in mean stress
3. An increase in PD OD correlates with a decrease in mean stress, and
4. An increase in BMD correlates with an increase in mean stress

The sample sizes for the degenerated study were too small for statistical analysis and therefore plotted graphs (See Figures 21-24) were used. None of the correlations listed above could be disputed as most of the plots showed similar trends. Model 1 tendons did not show any correlation.

There is a potential with these correlations to improve the clinical management of Achilles tendons after injury or repair. It is hypothesized (C) that a mathematical model could be developed that can predict load tolerances by correlating optical densities with mean stress. This mathematical model would then use the approximated mean stress and measured cross-sectional area to determine the peak tolerable load before rupture and thus determine the amount of physical activity permitted.

## 6.5 Comparison of Experimental Achilles Tendon Models with Human Achilles Tendons

Both healthy and degenerated tendons recovered their complete mechanical strength by four weeks, but human tendons are thought to take up to twenty-six weeks to heal. Three possible causes for the inconsistency between our models and humans, are that:

- 1) Our model fails to properly model or simulate human injury and degeneration,
- 2) Our models are accurate and humans also recover their tendon mechanical strengths early after surgery, and/or
- 3) The inconsistency between the rabbit models is the result of immediate return to weight bearing activity, when humans are immobilized for up to six weeks.

*Cause 1:* As all other data (cross-sectional area, ODs, Stress) is in accordance with human results, it is unlikely that our model is a complete failure. If improvements are necessary, the method of causing degeneration should be validated and/or improved. It is currently unknown whether or not reducing the blood flow in the tendons actually causes damage to the collagen fibers. Collagen is very resilient and if the collagen is not being affected by the ischemia then degeneration of the mechanical properties will not occur.

*Cause 2:* Assuming our models have provided an adequate representation of human Achilles tendons, then it appears that human tendons may actually recover mechanical strength sooner after injury, and that imaging results are more indicative of mean stress than mechanical strength. This would mean that patients could

return to regular activity sooner than originally thought.

*Cause 3:* The rabbit Achilles tendons in these studies were allowed unrestricted movement (with pain treatment) after surgery, which opposes current human clinical management of tendon injury. Human tendons are immobilized up to six weeks after a major injury or surgery. Allowing weight bearing activity after injury (in our models), may have increased the rate of rabbit Achilles tendon recovery of mechanical strength. Tendon strength depends of the collagen strength and orientation. These variables are based on the load demands of the tendon. If the load demands are not present, than the collagen fiber turn over rate increases and the fiber orientation becomes nonuniform as seen in several immobilization studies [12] [13] [15] [16]. Immobilization after repair may actually slow down the recovery rate since very little mechanical demand needs to be met. This study hypothesizes (B) that return to load bearing activity sooner after injury or repair, increases the rate of mechanical strength recovery.

## Chapter 7

# Design for Continued Study/Future Work

Three hypotheses have been developed from the cumulative results provided in both rabbit Achilles tendon studies.

- A) Tendons recover mechanical strength early after injury or surgical repair, and this recovery is accomplished by increasing the cross-sectional area and thus reducing stress
- B) Return to load-bearing activity sooner after injury or repair increases the rate of mechanical strength recovery
- C) There is a correlation between peak mean stress and optical density, and a mathematical model could be used to approximate the percent recovery of tendon strength based on the observed optical density.

This chapter describes these hypotheses in more details and proposes how the studies could be conducted and applied to clinical management of human tendons.

## 7.1 Hypothesis A

### **Tendons recover mechanical strength early after injury or surgical repair**

Despite degeneration, the mechanical strength of the rabbit Achilles tendons recovered by four weeks while the imaging results continued to show abnormalities. The return to peak load capacity was accompanied by an increase in cross-sectional area and decrease in stress.

It was first hypothesized in the previous study [1] that human tendons also recover mechanical strength earlier than currently expected and that this recovery may be attributed to an increase in cross-sectional area, thus a decrease in stress. This decrease in stress is believed to allow tendons to withstand normal load requirements soon after injury. Clinical human studies indicate that tendons heal much slower than the four weeks observed in this study; however, it is unknown how fast the mechanical strength is recovered. The rate of healing has been quantitated by several factors that do not actually measure the mechanical strength. Examples of factors thought to represent healing are pain relief, inflammation, range of plantar motion, quality of life, etc. Our results do not refute these factors as indicators of healing. They do however, raise the question: Is the mechanical strength of tendons recovered before healing (by clinical standards) is complete?

One human study allowed load bearing as early as 2 weeks after surgical repair with no cases of re-rupture [48]. This indicates that the hypothesis is worth investigating. Early weight bearing may also have beneficial effects on tendons strength recovery.

## 7.2 Hypothesis B

### **Return to load-bearing activity sooner increases the rate of mechanical strength recovery**

The rabbits in our models were allowed unrestricted movement whereas human tendons are usually immobilized after major injury, or repair. Our tendon models recovered their mechanical strength much faster than human tendons are predicted to therefore it is hypothesized that return to load-bearing activity soon after injury may increase the rate of mechanical strength recovery.

Previous studies have investigated the effects of immobilization on healthy tendons [15] and found a decrease in calcaneal BMD which resulted in failure at the bone insertion. Matsumoto *et al.* suggested that isolation of the tendons was necessary to see the effect of immobilization on tendons since all failures in their study occurred at the site of calcaneal insertion.

More recent studies have investigated the effects of early weight-bearing and immobilization on tendons after surgical repair [13] [14] [48] [49]. These studies indicate that immobilization after surgery causes undesired muscle atrophy, weaker tendon healing due to random orientation of the collagen, longer rehabilitation times, and a delay of mechanical strength recovery. In all studies weight-bearing tendons showed improved healing and no evidence that early weight-bearing increased the risk of re-injury.

It is believed that early weight-bearing (mobilization) stimulates the intrinsic healing response of the tendon and increases collagen orientation. The results are

stronger tendon healing and limited muscle atrophy.

To test this hypothesis, a comparison study between tendons that are immobilized and tendons that are allowed unrestricted motion after acute injury or repair is required. The goal of this comparison would be to prove that mobilized tendons recover their mechanical strength faster than tendons that are immobilized.

### 7.3 Hypothesis C

**There is a correlation between peak mean stress and optical density, and a mathematical model could be used to approximate the percent recovery of tendon strength based on the observed optical density**

A mathematical model correlating the MR optical densities and cross-sectional area to the mean peak stress could allow physicians to predict the maximum allowable tendon load before rupture. The estimated peak load to failure can then be calculated by multiplying the mean stress with the cross-sectional area.

Our study indicates that there is a correlation between optical density and peak mean stress: however, the exact correlation has yet to be developed. A large animal study designed to evaluate the correlation between peak stress and optical density is required to develop a mathematical correlation. Many contributing factors would have to be considered. Examples of these factors are the severity of the tendon injury, mode of injury, and tendon health prior to injury. There currently exist no method of accurately measuring the mechanical strength of human Achilles tendons *in vivo*. Extensive verification of the animal mathematical correlation would be required before

it could be adapted for humans. Validation of the animal mathematical model would include comparison of results obtained using the model to those obtained through mechanical testing. In applying a correlation to humans, many new contributing factors will have to be considered (age, sex, race, activity level, ect.).

## **7.4 Contributions and Future Work**

In summary, our study has lead to one new possible areas of research and supported two others. We did not find any investigation linking early mechanical strength recovery with a mathematical correlation to allow tendon strength prediction. Our results also support recent publications showing that cross-sectional area increases as a means of recovering mechanical strength and that load bearing activity soon after repair increases the rate of mechanical strength recovery and does not increase the risk of re-injury.

These new areas will require extensive research and testing before they can be applied to humans. In order to accurately, reproducibly, and efficiently mechanically test tendons for these studies a more time efficient mechanical testing assembly is necessary.

## Chapter 8

# Mechanical Testing Equipment Analysis

This chapter explains in more detail the mechanical testing equipment used in this study, evaluates it, and recommends possible improvements.

## 8.1 Current Equipment

A Dual Cryogenic Fixation System (DCF) (designed by Nanthan Ramachandran at the Ottawa University Bone and Joint Laboratory [31]) was used to mechanically test the specimens in this study. This fixation system is unique because it tests the tendons in isolation. By isolating the tendon, rupture at the midsection rather than at the bone insertion is achieved. This allows the strength of the tendons to be tested rather than the strength of tendon-bone insertion, clamp, or muscle-tendon insertion. As a result, larger peak loads have been obtained using this system compared to previously documented values.

### 8.1.1 Components of the Dual Cryogenic Fixation System

The DCF consists of two nearly identical cryofixations, two insulators, and a heater. The cryofixations comprise an inner test area (ice container), that holds

the specimens and saline solution, and an outer chamber ( $N_2$  chamber) that allows circulation of liquid nitrogen ( $N_2$ ) around the inner test area. The circulating  $N_2$  freezes the contents of the test area. The complete DCF system is illustrated in Figure 25.

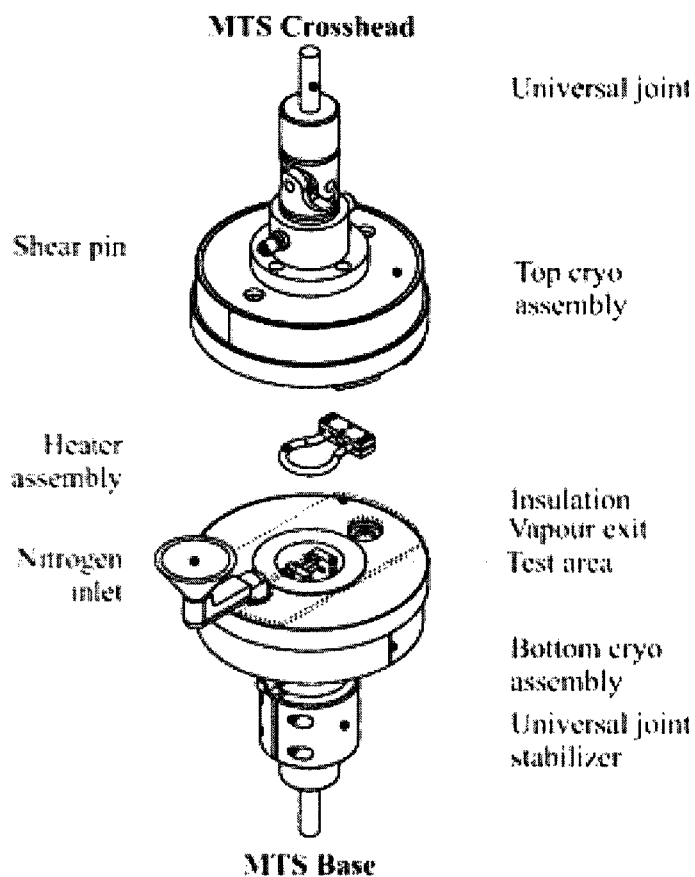


**Figure 25:** The complete Cryofixation setup [31].

The test area, illustrated in Figure 26 contains two aluminum support rods and two stainless steel alignment rods. The top alignment rod positions the tendon in the centre of the test area and the bottom alignment rod (spring loaded) presses against the specimen aligning it perpendicular to the surface of the cryo-fixation. This alignment reduces any strain on the ice surface resulting from misalignment

while the specimen is under load. The top fixation is slightly modified (it does not have a spring loaded bar, but rather a stationary bar) to accommodate for the bone-tendon complex.

Surrounding the test area (ice chamber) is the aluminum  $N_2$  chamber. The purpose of this chamber is to house the circulating liquid nitrogen while it freezes the saline solution in the test area. The chamber is insulated by polyurethane foam to increase the thermal capacitance. Two holes in the top of the chamber make up the inlet and exit. The exit hole provides an exit for the vaporized liquid nitrogen and relieves pressure inside the chamber.

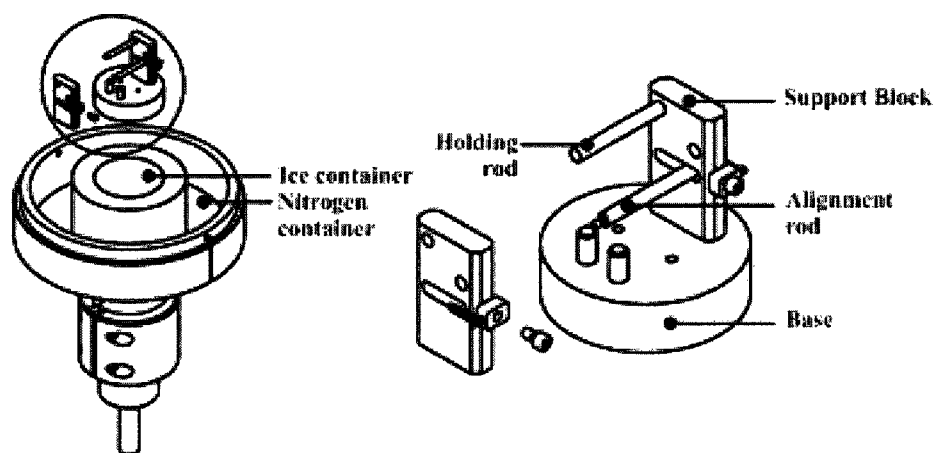


**Figure 26:** Assembly of the bottom fixation [31]

The final components of the DCF system are the heater and insulators. As seen in Figure 25, the heater is centered between the cryofixations and surrounds the specimen. The purpose of the heater is to ensure the midsection of the tendon is at body temperature. To prevent melting of the ice surface insulators were placed over the ice surfaces of each fixation. This setup successfully achieves a sharp temperature

gradient along the length of the specimen.

### **8.1.2 Evaluation of Design**

This cryofixation design is unique because it isolates the tendon specimen and allows for mechanical testing of the tendon only. The concept of using cryogenic fixations allows for a uniform distribution of the load across the cross-section of the specimen. It also prevents stress concentrations, slippage, and failure at the fixations. There are however, some areas of this design that require improvement. These improvements include reducing the freezing time, increasing accessibility of the tendon in the fixation device, and providing better thermal maintenance.

#### **Fixation freezing time**

A more time efficient method of freezing the fixations is required. The current design involves pouring liquid nitrogen into the N<sub>2</sub> chamber to freeze the saline filled test areas that hold the specimens ends. This freezing takes about 20 minutes per fixation. An optimized freezing schedule was created to eliminate over and under freezing. It requires that the top fixation be frozen first and mounted on the MTS crosshead before the specimen can be lowered into the bottom fixation. Saline solution is then added to the bottom fixation test area and the specimen threaded through the bottom fixation alignment rods. Once the muscle-tendon complex is secured by the bottom fixation alignment rods, the liquid nitrogen is added to the bottom N<sub>2</sub> chamber and the bottom test area is frozen. In order to maintain the correct ice and tendon midsection temperatures, during the mounting of the tendons and the fixations, a total of 50 minutes and 1.4 L of liquid Nitrogen is required. 50 minutes to prepare for mechanical testing is a substantial amount of

time when hundreds of mechanical tests may be required. The longer the fixation time required, the higher the risk is that the properties of the tendon will be negatively affected. The mechanical testing itself takes no longer than 5 minutes. As a results, reducing the freezing time would substantially decrease the amount of time it takes to mechanically test a specimen and many more tendons could be accurately tested. There would also be less chance of changing the tendons properties.

### **Accessibility**

Accessibility is an issue due to the fixation size required for the N<sub>2</sub> freezing method. The large outer diameter of the fixations and the small gauge length of the specimens leaves very little room to access the specimen during fixation and mechanical testing. In addition, the heater also takes up the bulk of the limited space. Since the gauge length is limited by the size of the specimen, a decrease in fixation size or change in fixation shape are the only way to increase accessibility to the specimen and test areas. The lack of access causes problems monitoring slip and makes fixation difficult.

Additional access is required to allow for a more accurate method of monitoring slip at the fixations. Validation that no slippage occurred during the mechanical loading is currently done by means of monitoring the load-displacement readout from the data acquisition system. Further verification of no slip is desired and the current DCF system has limited room between fixations for other means of monitoring slip. The recommended means of monitoring slip and displacement of the fixations, is to use a video displacement system. This system would require access to the fixated specimen along the gauge length during the entire mechanical test.

Improvement to the access is necessary to ease fixation of the specimen in the

bottom fixation. To fix the muscle-tendon complex in the bottom fixation, a suture tied to the muscle portion of the specimen is threaded through the alignment rods of the bottom fixation. The suture is then pulled while the MTS cross-head and top fixation are lowered. The end result is a 25 mm gauge length with the muscle-tendon complex wrapped around the alignment rods and submerged in saline solution. At this point, additional saline solution is added, by means of a dropper, to the bottom test area. The limited space between fixations makes adding the saline solution difficult and time consuming. The additional time interferes with the optimized freezing schedule which has negative implications.

### **Thermal control**

A freezing method that allows for better thermal control is required to prevent failure at the fixation. The optimized freezing schedule leaves very little room for error and any fluctuations in ice temperature weakens the ice causing failure at the fixation rather than at the midsection of the specimen. The thermal components (heater, insulators, and liquid nitrogen) also require improvements to ensure the proper control of the temperature gradient.

The optimized freezing schedule leaves very little room for error. If any of the steps go beyond the allotted time, the schedule no longer applies. As soon as any delay occurs, the remainder of the freezing protocol must be estimated. For example, if there are any difficulties threading the muscle-tendon complex through the alignment rods of the bottom fixation, then elapsed time will interfere with the optimized schedule. Maintaining the appropriate top fixation ice temperature will now require monitoring of the ice temperature (using the thermocouples) and estimation of the amount of liquid N<sub>2</sub> required to bring the ice back to the correct

temperature. Any errors in estimation causes unwanted changes in ice temperature, often outside the appropriate temperature range. Ice temperatures that are too high can cause cracking of the ice surface as it expands, weakening the ice. Low ice temperatures cause poor adhesion and leave the potential for slippage at the fixation.

The current method of controlling the temperature gradient is also problematic. The sharp temperature gradient is achieved using a heater at the midsection of the specimen (at half of the gauge length), with insulators at the ice surfaces. The N<sub>2</sub> inlet is positioned very close to the specimen. As the liquid nitrogen is added to the N<sub>2</sub> chamber, N<sub>2</sub> vapours surround the specimen gauge length decreasing its temperature and interfering with the very important temperature gradient. Every time liquid nitrogen is added, the mid section temperature decreases significantly and time is required for the specimen to reheat to body temperature (37°C). If the tendon is not at body temperature during the mechanical loading, the mechanical results obtained will be invalid. This temperature adjustment further complicates the freezing process if any deviation from the optimized freezing schedule occurs.

## 8.2 Suggested Design Improvements

In summary, the freezing method needs improvement. The liquid nitrogen freezing method takes too long to freeze the fixations, leaves very little room for access to the test area and specimen, and doesn't allow for adequate thermal control.

As previously mentioned, decreasing the diameter of the fixations or changing the shape (ex. conical) will increase the accessibility of the specimen and test areas. Investigation into possible fixation shapes is recommended to increase access. Gained

accessibly will allow the displacement and slippage to be monitored using a video displacement system and improve the ease of fixing the muscle-tendon complex in the bottom fixation.

The new design should also include a method of freezing the fixations in a much shorter time, minimize any temperature fluctuations in the mid-section of the specimen, and not include a freezing protocol that is so sensitive to change.

L. Rincon *et. al* designed a successful cryogenic fixation device that could be adapted to this application. The design consisted of two solid aluminum blocks (80 x 50 x 40 mm) with a half cylindrical 25 mm diameter hole machined along the side of each [21]. The cylinders were cooled in liquid nitrogen and wrapped around a cylindrical core test area. They were able to cool the aluminum blocks to  $-196^{\circ}\text{C}$  in about 10 minutes. Water was then poured into the core (test area) along with the specimen, where it was instantly frozen. The second portion of their study described the temperature profile within the tissue of porcine tendons for different initial aluminum block temperatures. The aluminum blocks were found to require a maximum freezing temperature of  $-30^{\circ}\text{C}$  to completely solidify the ice core (test area).

Using solid aluminum blocks, as Rincon did, rather than  $\text{N}_2$  chambers to freeze the test area shows promise to reduce the freezing and fixation times, decrease the size of the fixations, and minimize any mid-section temperature changes. By decreasing the freezing time, it is also believed that the freezing protocol will not be as affected by time constraints. An optimal initial aluminum block temperature that allows for the allotted time to mount the fixations would need to be calculated and tested experimentally.

The new cryofixation design would adapt Rincons design to satisfy our requirements: to test the specimens in isolation, and maintain adequate thermal control. Rincons design consists of one cryofixation and relies on the bony attachment to the tendon for the second fixation. It was also designed for larger specimens which meant that the distance, between the midsection of the specimen and the ice, was large enough to reduce heat transfer. To allow for tendon isolation, this design would have to be adapted to consist of two fixations. The addition of a second fixation makes thermal control more difficult.

An improved thermal control system is necessary. Any heat transfer between the ice and the specimen affects the temperature of the tendon at midsection. Our specimens are much smaller than Rincon's and heat transfer would occur between the two clamps and the specimen. A radiant light source and reflective insulators are recommended to heat the tendon and maintain ice temperature without decreasing access to the specimen. This mode of maintaining thermal control is possible with the reduction of the fixation size.

In conclusion, an adaptation of Rincons design will reduce the freezing time, increase access to the specimen and test area, and has the potential to increase thermal control.

## Chapter 9

# Conclusions and Future Research

The study in this thesis was designed to investigate the hypothesis that tendons with pre-existing degeneration recover their mechanical properties slower after injury compared to healthy tendons. This hypothesis was formed based on previous work done on healthy tendons with the same acute injury. Two rabbit Achilles tendon models were tested: Model 1 - degeneration due to ischemia, Model 2 - degeneration due to ischemia followed by an acute partial tendon tear. Rabbits were euthanized at either 2 or 4 weeks after surgery. The rabbit tendons were then imaged (MRI, US, and BMD) and mechanically tested for peak load to failure.

The conclusions of the experimental study, the evaluation of the mechanical testing equipment, and suggestions for future research are presented below.

### 9.1 Experimental Study Conclusions

Our hypothesis was refuted according to the data available in this study. Tendons with degeneration did not recover their mechanical strength slower than the healthy tendons with the same acute injury. The mechanical strength recovered by as much

as 80% at 2 weeks and fully by 4 weeks, in both models.

Despite mechanical strength recovery, the imaging results and reduction in stress indicate that the degenerated tendons do heal slower than the healthy tendons with the same injury. The degenerated-injured tendons were 78% larger than the healthy-injured tendons at 2 weeks and 22% larger at 4 weeks. All T1 weighted, PD, and T2 weighted optical densities were also approximately 40% higher in the degenerated-injured tendons than in the healthy-injured tendons. The peak mean stress in the degenerated-injured tendons was only 22% and 90% of that of the healthy-injured tendons at 2 weeks and 4 weeks, respectively. It is believed that an increase in cross-sectional size and decrease in peak stress allows the tendons as a whole to withstand the same peak loads soon after injury.

It remains undetermined whether or not degeneration was achieved by means of strangulation (Model 1). Imaging results (MRI & US) showed an increase in cross-sectional area which is indicative of degeneration, however the mechanical strength recovered 80% of its strength by two weeks and fully recovered by four weeks. The peak mean stress in the strangulated tendons did however, decrease substantially. Histological assessment is required to verify degeneration in this model.

Our study supports the hypothesis that there exists a correlation between peak mean stress and optical density and this correlation could be used to predict peak load to failure. Peak load to failure is calculated by multiplying the peak mean stress by the measured cross-sectional area of the tendon.

## 9.2 Evaluation of Mechanical Testing Equipment

There are three issues with the dual cryogenic fixation system: long fixation time, poor access to the specimen and test area, and inadequate thermal control. Long fixation time limits the number of mechanical tests possible in a day. Poor access causes difficulties with clamping and limits the method of monitoring slip. Inadequate thermal control increases the risk of failure at the fixation and causes the tendon specimen to fluctuate in temperature.

A new method of freezing the fixations could solve these issues. A design is proposed that includes using aluminum blocks submerged in liquid nitrogen, as conducted by Rincon *et al.*, as the method of freezing the fixations. This design has the potential to reduce the freezing time from 50 minutes to 10 minutes, increase the access to the specimen and test area, and increase thermal control.

## 9.3 Future Research

Further study is necessary to test the following hypotheses for humans : A) tendons recover mechanical strength early after injury or surgical repair, and this recovery is accomplished by increasing the cross-sectional area and thus reducing stress, B) return to load-bearing activity sooner after injury or repair increases the rate of mechanical strength recovery, and C) a mathematical model could correlate mean stress with optical density, and could be used to approximate the percent recovery of tendon strength.

The results show a potential to improve the treatment of Achilles tendons after

injury or surgical repair. Current treatment involves immobilization of the foot for up to 6 weeks before slowly re-introducing weight bearing activity. Recommending reduced mobility after injury or repair may be detrimental. Studies have shown that immobilization of tendons causes increased collagen fibre turnover, non-uniform orientation, and therefore a decrease in mechanical strength. The results from this study show that the occurrence of an increase in cross-sectional area reduces stress, and allows the tendons to withstand normal peak loads early after injury. As a result, a return to regular activity sooner after injury or repair, rather than later, may improve the collagen orientation and strength, and reduce recovery time.

There is also a potential to improve clinical management after injury or repair, by correlating imaging results with the mechanical load tolerance of the tendons. This study and previous work have shown that a potential correlation between mean stress and optical density exists. Through this correlation, the load tolerance of the tendons could be determined using the cross-sectional area measurement. To properly correlate the mean stress and optical density, a mathematical model is necessary.

## List of References

- [1] G. Trudel, G. P. Doherty, Y. Koike, N. Ramachandran, M. Lecompte, L. Dinh, and H. K. Uhthoff, "Restoration of strength despite low stress and abnormal imaging after achilles injury," *Medicine & Science in Sports & Exercise*, In Press.
- [2] NASA, "Anthrometric source book." <http://msis.jsc.nasa.gov/sections/section03.htm>, 2008.
- [3] E. N. Marieb, *Human Anatomy and Physiology*, pp. 14–16. The Benjamin/Cummings Publishing Company, Inc., 3rd ed., 1995.
- [4] W. E. Erkonen and W. L. Smith, *Radiology 101: The Basics and Fundamentals of Imaging*. Lippincott Williams and Wilkins, 2nd ed., 2005.
- [5] Radiological Society of North America, Inc., "Bone Density Scan." <http://www.radiologyinfo.org/>, 2009.
- [6] A. D. Tabensky, J. Williams, V. Deluca, E. Briganti, and E. Seeman, "Bone mass, areal, and volumetric bone density are equally accurate, sensitive, and specific surrogates of the breaking strength of the vertebral body: An in vitro study," *Journal of Bone and Mineral Research*, vol. 11, no. 12, pp. 1981–1988, 1996.
- [7] M. M. Sran, K. M. Khan, K. Keiver, J. B. Chew, H. A. McKay, and T. R. Oxland, "Accuracy of DXA scanning of the thoracic spine: Cadaveric studies comparing BMC, areal BMD and geometric estimates of volumetric BMD against ash weight and CT measures of bone volume," *European Spine Journal*, vol. 14, no. 10, pp. 971–976, 2005.
- [8] Y. Koike, H. K. Uhthoff, N. Ramachandran, G. P. Doherty, M. Lecompte, D. S. Backman, and G. Trudel, "Achilles tendinopathy," *Critical Reviews in Physical and Rehabilitation Medicine*, vol. 16, no. 2, 2004.

- [9] Griffin Global Systems, “Everything about achilles tendons.” <http://www.achillestendon.com/>, July 2009.
- [10] W. B. Leadbetter and N. R. Maffulli, “Tendon injuries: Basic science and clinical medicine,” 2005.
- [11] C. R. Ethier and C. A. Simmons, *Introduction to Biomechanics From Cells to Organisms*, pp. 29–35. Cambridge University Press, 2007.
- [12] C. N. Maganaris and M. V. Narici, *Tendon Injuries: Basic Science and Clinical Medicine*, pp. 14–21. Springer, 2005.
- [13] N. Maffulli, C. Tallon, J. Wong, K. P. Lim, and R. Bleakney, “Early weight-bearing and ankle mobilization after open repair of acute midsubstance tears of the achilles tendon,” *American Journal of Sports Medicine*, vol. 31, no. 5, pp. 692–700, 2003.
- [14] M. Speck and K. Klaue, “Early full weightbearing and functional treatment after surgical repair of acute achilles tendon rupture,” *American Journal of Sports Medicine*, vol. 26, no. 6, pp. 789–793, 1998.
- [15] F. Matsumoto, G. Trudel, H. K. Uthoff, and D. S. Backman, “Mechanical effects of immobilization on the achilles tendon,” *Archives of Physical Medicine and Rehabilitation*, vol. 84, no. 5, pp. 662–667, 2003.
- [16] T. Yasuda, M. Kinoshita, M. Abe, and Y. Shibayama, “Unfavorable effect of knee immobilization on achilles tendon healing in rabbits,” *Acta Orthopaedica Scandinavica*, vol. 71, no. 1, pp. 69–73, 2000.
- [17] C. A. Soma and B. R. Mandelbaum, “Repair of acute achilles tendon ruptures,” *Orthopedic Clinics of North America*, vol. 26, no. 2, pp. 239–247, 1995.
- [18] B. Abelson, “Injuries to the achilles tenon.” <http://www.drabelson.com>, July 2009.
- [19] D. Kader, M. Mosconi, F. Benazzo, and N. Maffulli, *Tendon Injuries: Basic Science and Clinical Medicine*, pp. 187–200. Springer, 2005.
- [20] M. Paavola, P. Kannus, and M. Jarvinen, *Tendon Injuries: Basic Science and Clinical Medicine*, pp. 32–39. Springer, 2005.
- [21] Worker’s Compensation Board, “Achilles tendon repair: Post-op rehabilitation guidelines.” <http://www.worksafefbc.com>, 2005.

- [22] University of Delaware Physical Therapy Clinic, "Rehab practice guidelines for: Achilles tendon repair." <http://www.udel.edu>, 2005.
- [23] S. J. Warden, "Animal models for the study of tendinopathy," *British Journal of Sports Medicine*, vol. 41, no. 4, pp. 232–240, 2007.
- [24] M. Jassem, A. T. Rose, K. Meister, P. A. Indelicato, and D. Wheeler, "Biomechanical analysis of the effect of varying suture pitch in tendon graft fixation," *American Journal of Sports Medicine*, vol. 29, no. 6, pp. 734–737, 2001.
- [25] H. Thermann, O. Frerichs, A. Biewener, and C. Krettek, "Healing of the achilles tendon: An experimental study," *Foot and Ankle International*, vol. 22, no. 6, pp. 478–483, 2001.
- [26] G. P. Doherty, Y. Koike, H. K. Uthoff, M. Lecompte, and G. Trudel, "Comparative anatomy of rabbit and human achilles tendons with magnetic resonance and ultrasound imaging," *Comparative Medicine*, vol. 56, no. 1, pp. 68–74, 2006.
- [27] R. R. Fox, "The rabbit as a research subject.," *Physiologist*, vol. 27, no. 6, pp. 393–402, 1984.
- [28] D. J. Riemersa and H. C. Schamhardt, "The cryo-jaw, a clamp designed for in vitro rheology studies of horse digital flexor tendons," *Journal of Biomechanics*, vol. 15, no. 8, pp. 619–620, 1982.
- [29] A. B. Liggins, R. Shemerluk, R. Hardie, and J. B. Finlay, "Technique for the application of physiological loading to soft tissue in vitro," *Journal of Biomedical Engineering*, vol. 14, no. 5, pp. 440–441, 1992.
- [30] L. S. e. a. L. Rincon, "Design and evaluation of a cryogenic soft tissue fixation device - load tolerances and thermal aspects," *Journal of Biomechanics*, vol. 34, pp. 393–397, 2001.
- [31] N. Ramachandran, Y. Koike, P. Poitras, D. Backman, H. K. Uthoff, and G. Trudel, "Dual cryogenic fixation for mechanical testing of soft musculoskeletal tissues," *IEEE Transactions on Biomedical Engineering*, vol. 52, no. 10, pp. 1792–1795, 2005.
- [32] L. Schatzmann, P. Brunner, and H. U. Stubli, "Effect of cyclic preconditioning on the tensile properties of human quadriceps tendons and patellar ligaments," *Knee Surgery, Sports Traumatology, Arthroscopy*, vol. 6, no. 1, 1998.

- [33] B. H. Ng, S. M. Chou, and V. Krishna, "The influence of gripping techniques on the tensile properties of tendons," *Proceedings of the Institution of Mechanical Engineers, Part H: Journal of Engineering in Medicine*, vol. 219, no. 5, pp. 349–354, 2005.
- [34] J. Lepetit, R. Favier, A. Grajales, and P. O. Skjervold, "A simple cryogenic holder for tensile testing of soft biological tissues," *Journal of Biomechanics*, vol. 37, no. 4, pp. 557–562, 2004.
- [35] N. A. Sharkey, T. S. Smith, and D. C. Lundmark, "Freeze clamping musculo-tendinous junctions for in vitro simulation of joint mechanics," *Journal of Biomechanics*, vol. 28, no. 5, pp. 631–635, 1995.
- [36] F. Morelli, A. Ferretti, F. Conteduca, F. Nanni, L. Monteleone, and M. Valente, "A modified cryo-jaw for in vitro biomechanical testing of tendons," *Journal of Applied Biomechanics*, vol. 18, no. 4, pp. 384–389, 2002.
- [37] P. Wieloch, G. Buchmann, W. Roth, and M. Rickert, "A cryo-jaw designed for in vitro tensile testing of the healing achilles tendons in rats," *Journal of Biomechanics*, vol. 37, no. 11, pp. 1719–1722, 2004.
- [38] D. L. Hamner, C. H. Brown Jr., M. E. Steiner, A. T. Hecker, and W. C. Hayes, "Hamstring tendon grafts for reconstruction of the anterior cruciate ligament: Biomechanical evaluation of the use of multiple strands and tensioning techniques," *Journal of Bone and Joint Surgery - Series A*, vol. 81, no. 4, pp. 549–557, 1999.
- [39] J. W. Miles, W. A. Grana, D. Egle, K. . Min, and J. Chitwood, "The effect of anabolic steroids on the biomechanical and histological properties of rat tendon," *Journal of Bone and Joint Surgery - Series A*, vol. 74, no. 3, pp. 411–422, 1992.
- [40] G. L. Matthews, K. G. Keegan, and H. L. Graham, "Effects of tendon grip technique (frozen versus unfrozen) on in vitro surface strain measurements of the equine deep digital flexor tendon," *American Journal of Veterinary Research*, vol. 57, no. 1, pp. 111–115, 1996.
- [41] E. Powell, I. Trail, and J. Noble, "Non-suture repair of tendons," *Journal of Biomedical Engineering*, vol. 11, pp. 215–218, 1989.
- [42] A. Probst, D. Palmes, H. Freise, M. Langer, A. Joist, and H. U. Spiegel, "A new clamping technique for biomechanical testing of tendons in small animals," *Journal of Investigative Surgery*, vol. 13, no. 6, pp. 313–318, 2000.

- [43] K. Hornbech Svendsen and G. Thomson, "A new clamping and stretching procedure for determination of collagen fiber stiffness and strength relations upon maturation," *Journal of Biomechanics*, vol. 17, no. 3, pp. 225–229, 1984.
- [44] J. Z. Wu, A. Brumfield, G. R. Miller, R. Metheny, and R. G. Cutlip, "Comparison of mechanical properties of rat tibialis anterior tendon evaluated using two different approaches," *Bio-Medical Materials and Engineering*, vol. 14, no. 1, pp. 13–22, 2004.
- [45] T. M. Best, A. Collins, E. G. Lilly, A. V. Seaber, R. Goldner, and G. A. C. Murrell, "Achilles tendon healing: A correlation between functional and mechanical performance in the rat," *Journal of Orthopaedic Research*, vol. 11, no. 6, pp. 897–906, 1993.
- [46] J. T. . Cheung and M. Zhang, "A serrated jaw clamp for tendon gripping," *Medical Engineering and Physics*, vol. 28, no. 4, pp. 379–382, 2006.
- [47] G. Trudel and H. Uthoff, "CIHR Research Grant Proposal: Tendons with pre-existing degeneration, how differently do they heal?," 2006.
- [48] A. A. Suchak, G. P. Bostick, L. A. Beaupr, D. C. Durand, and N. M. Jomha, "The influence of early weight-bearing compared with non-weight-bearing after surgical repair of the achilles tendon," *Journal of Bone and Joint Surgery - Series A*, vol. 90, no. 9, pp. 1876–1883, 2008.
- [49] M. Majewski, S. Schaeren, U. Kohlhaas, and P. E. Ochsner, "Postoperative rehabilitation after percutaneous achilles tendon repair: Early functional therapy versus cast immobilization," *Disability and Rehabilitation*, vol. 30, no. 20-22, pp. 1726–1732, 2008.

## Appendix A

# Protocol: Mechanical Testing of Achilles Tendon

### A.1 Preparation

The following procedures are done prior to fixation of the specimen in the dual cryogenic fixation system.

#### A.1.1 Specimen preparation

In order to prepare the tendons for mechanical testing the following procedures are conducted:

1. Frozen tendons are thawed in water, at room temperature, for approximately 30 minutes or until completely thawed.
2. Three sutures are tied around the tendon to indicate the area of mechanical testing (gauge length) as well as the ice limits. The location of the sutures are indicated by points a, b, and c in Figure 1.
  - (a) Tie suture a around insertion point (the connection between calcaneus bone and tendon);

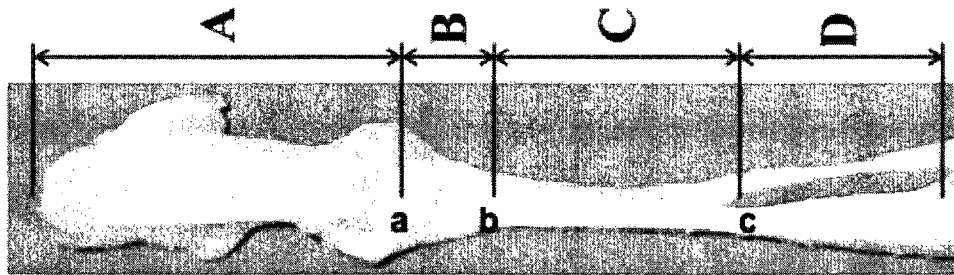


**Figure 27:** Rabbit Achilles Tendon. Length A represents the calcaneus bone area that is frozen along with length B in the TOP ice container. Point a is the insertion point. Point b is 10 mm from the insertion point and marks the beginning of the gauge length and ice limit. Point c is 25 mm from point b and marks the end of the the gauge length and second ice limit. Length D represents the proximal area frozen in the BOTTOM fixation. At the end of length D, a fourth suture is attached to allow for threading through the BOTTOM ice chamber. [31]

- (b) Tie suture b 10 mm proximal to the insertion (suture a);
  - (c) Tie suture c 35 mm proximal to the insertion (suture a);
3. A fourth suture is used to guide the proximal portion of the tendon (Length D in Figure 1), through the two rods in the BOTTOM ice container. The suture is tied at 20 mm proximal to suture c and approximately 127 mm of excess suture material is left for handling.
  4. Using Indian dye, paint the side of the tendon. This will help maintain the orientation of the tendon after rupture.
  5. For transportation or re-freezing, the tendons are wrapped in gauze and soaked in 1.0 percent saline solution and placed in a plastic bag.

### A.1.2 Dual cryogenic fixation assembly

The cryogenic fixation components are assembled for use. The schematic drawings for assembly are as follows:

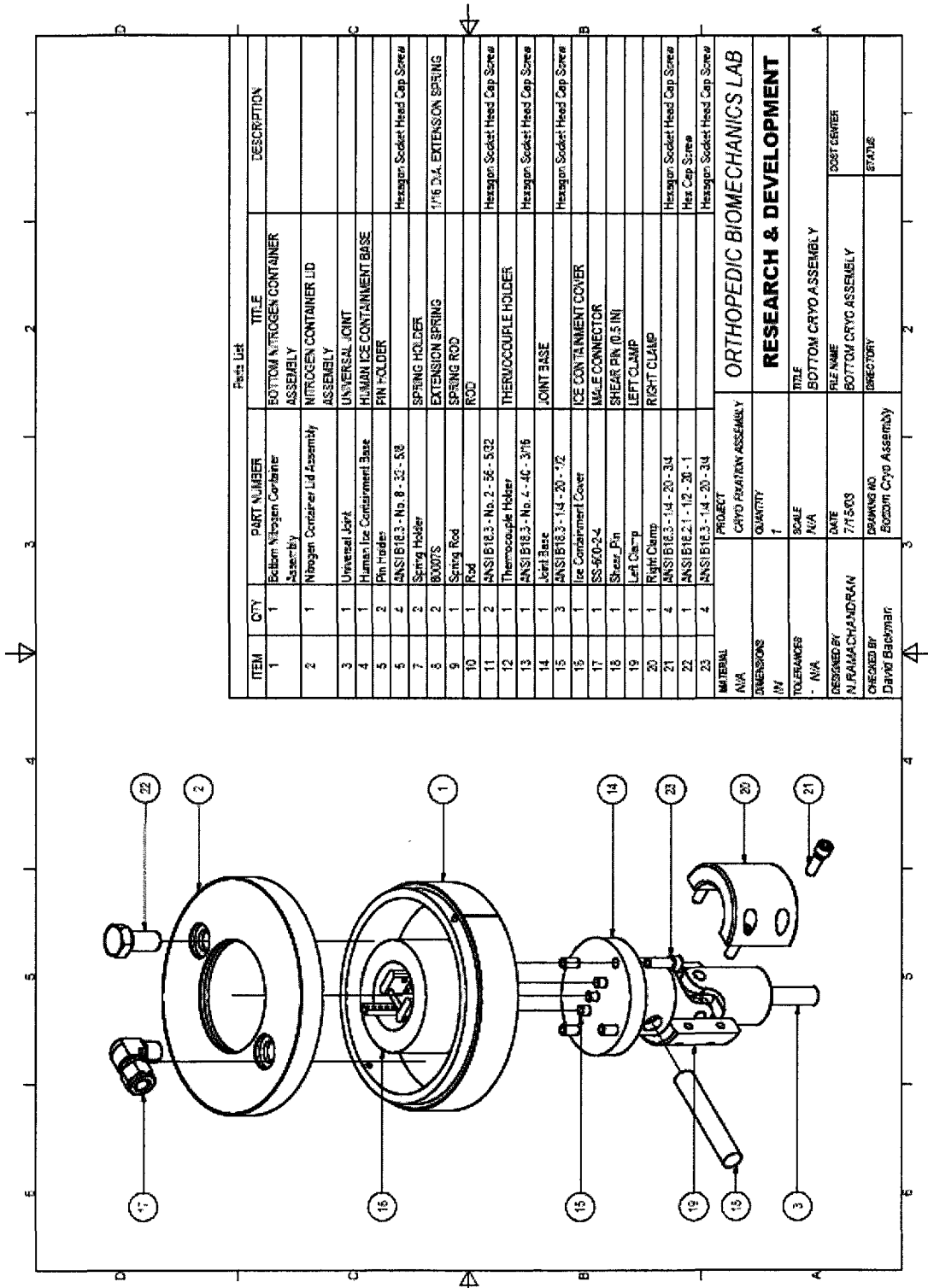


Figure 28: Fixation assembly Drawing Part 1 [31]

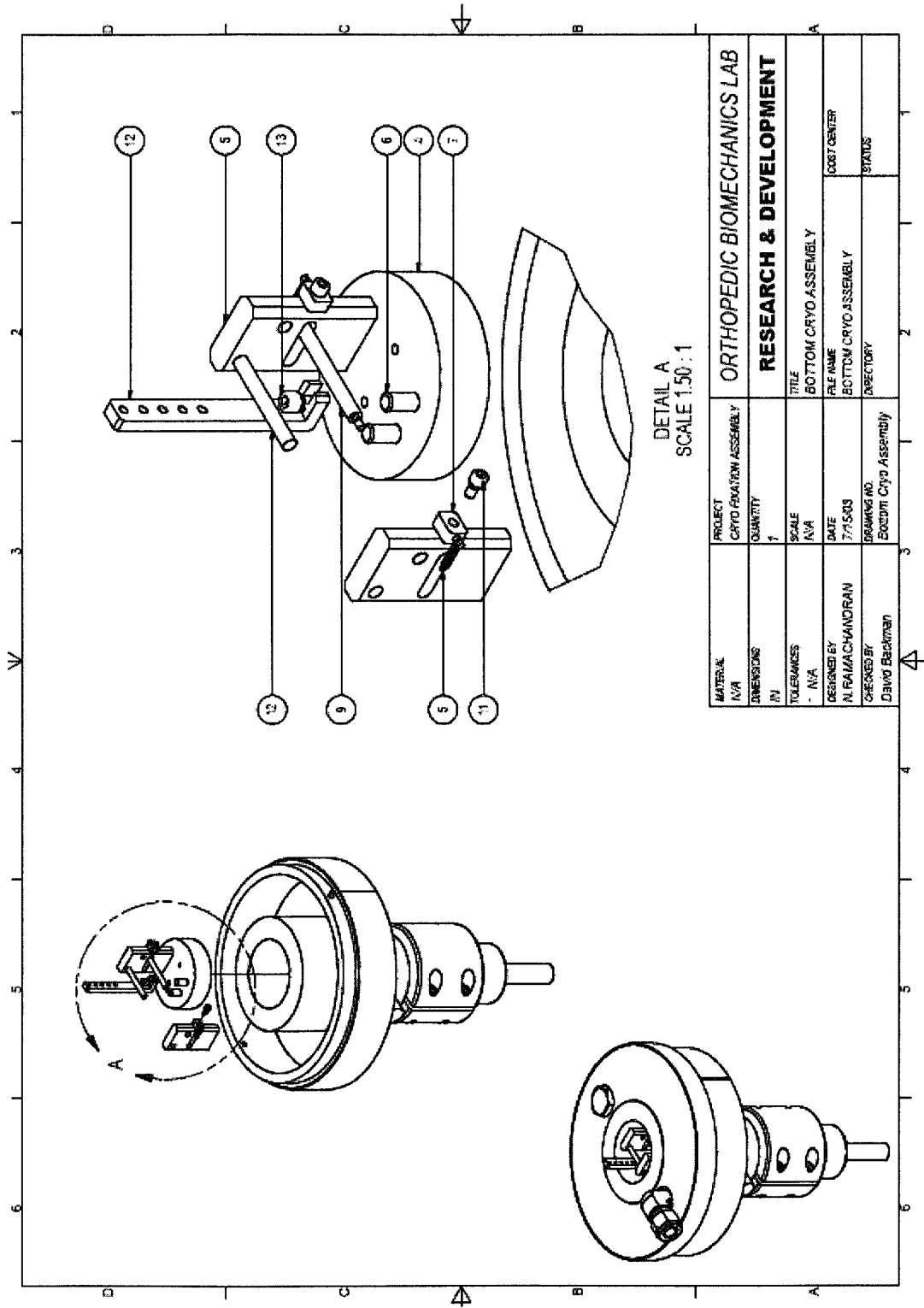


Figure 29: Fixation assembly Drawing Part 2 [31]

### **A.1.3 Thermometer set-up**

The temperature of ice 10 mm below the ice surface is monitored and recorded throughout the experiment. At the beginning of each test the MONARCH 309 thermometer is initialized as follows:

1. The thermometer is connected to the computer and two K-type thermocouples are attached.
2. The software, SE 309 - Test Link is started and the connection between thermometer and computer is verified.
3. Specimen fixing procedures further outline the steps required to monitor the temperature of the ice through out testing.

## **A.2 Specimen Fixing**

The following protocol outlines the mounting of the tendon in the dual cryogenic fixation system.

### **A.2.1 Freezing TOP fixation**

1. The distal portion of the Achilles tendon is placed between the holding rods in the TOP cryogenic fixation.
2. 0.1% Saline solution is poured into the ice container to the level indicated by suture b.
3. The handling suture is used in conjunction with a fixation and stand to hold the tendon vertically in position during the freezing of the TOP fixation.

4. One of the K-type thermocouples is then placed 10 mm below the saline level and affixed to the fixation with tape.
5. At  $t$  (with  $t$ = Test Start Time), 250 mL of  $N_2$  is added to the TOP Nitrogen container. (Note: A pipette is used to remove excess saline solution as freezing causes expansion).(Recording of the temperatures start)
6. At  $t+5$ , an additional 250 mL of  $N_2$  is added to the TOP Nitrogen container.
7. Cardboard insulator is then fixed to the fixation, using tape, covering the ice surface.

### **A.2.2 Mounting fixations**

1. At  $t+10$ , the handling suture is removed from the stand and the TOP fixation is attached to the MTS Crosshead.
2. The plugging bolts from the bottom of the TOP nitrogen container are removed and screwed into the top of the TOP nitrogen container.
3. The BOTTOM fixation is then mounted to the MTS Base.
4. The MTS Crosshead is lowered while the handling suture is thread through the BOTTOM ice container bars.
5. 0.1percent saline solution is poured into the BOTTOM ice container until it is approximately 3/4 full.
6. The second thermocouple is then taped to the BOTTOM fixation, allowing it to be submerged into the saline solution, 10 mm below suture c.
7. The MTS Crosshead is finally continuously lowered until the proximal portion of the tendon, (Length D, ending at suture c) is submerged in the saline solution.

Once in place the suture is taped to the fixation to maintain tension and ensure alignment of the tendon. If saline solution levels are too high, the pipette is used to gradually remove the fluid.

### **A.2.3 Freezing BOTTOM fixation**

1. At  $t+20$ , 250 mL of  $N_2$  is added to the BOTTOM Nitrogen container. (Note: A pipette is used to remove excess saline solution as freezing causes expansion).
2. At  $t+25$ , additional 250 mL of  $N_2$  is added to the BOTTOM Nitrogen container.
3. The second insulator is placed over the ice area.
4. The tendon is lubricated with petroleum jelly and the heater is placed around the tendon at a temperature of  $36^\circ\text{C}$ .

## **A.3 Mechanical Testing**

Continuous freezing, pre-loading and a final peak-load to failure test, comprise the mechanical testing of the Achilles tendons.

### **A.3.1 Maintaining the temperature of the cryogenic fixations while obtaining desired temperature gradient in the tendon**

1. At  $t+30$ , 100 mL of  $N_2$  is added to the TOP chamber.
2. At  $t+35$ , 100 mL of  $N_2$  is added to the BOTTOM chamber.
3. At  $t+40$ , 50 mL of  $N_2$  is added to the TOP chamber.
4. At  $t+45$ , 50 mL of  $N_2$  is added to the TOP and BOTTOM chambers.

5. At  $t+50$ , 50 mL of  $N_2$  is added to the BOTTOM chamber.

### **A.3.2 Pre-loading**

1. At  $t+50$ , the loading frame is calibrated to 5 kN. It is insure that there is no load on the frame for calibration.
2. The rabbit Achilles tendon - preconditioning method is opened and started.

### **A.3.3 Peak-load to failure**

1. At  $t+55$ , the rabbit Achilles tendon - Failure method is opened and started.

## **A.4 Histology Preparation**

In order to maintain the orientation of the tendon after rupture, the specimen must be mounted and aligned. The following steps are required:

1. Place the tendon on the tongue depressor, lying it flat and aligning the tendon ruptures with the dyed area facing upwards.
2. Place two holding pins through the tendon into the tongue depressor. The first one should be within Length B, ad the second within Length D.
3. Tie two sutures between Length B and Length D, holding the ruptured tendon pieces together in alignment.

# Appendix B

## Experimental Summary Process Map

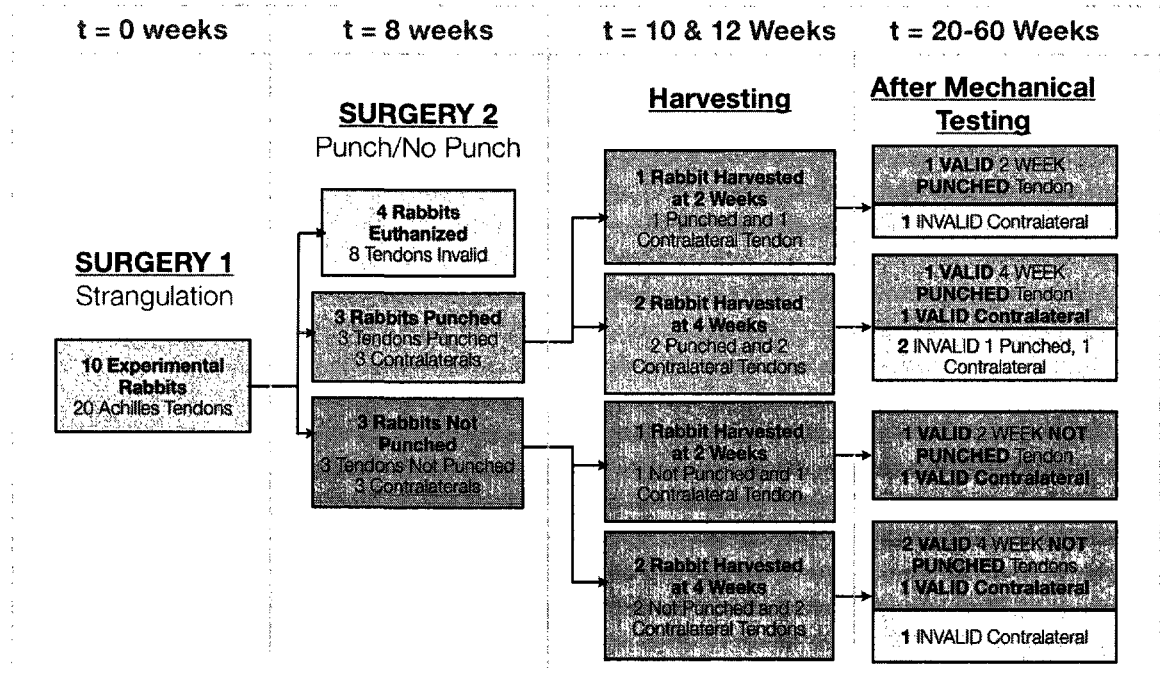


Figure 30: Process Map Summarizing the Experimental Procedures

## Appendix C

# Experimental Results

## C.1 Imaging Results

**Table 6:** Ultrasound Results for All Tendons

Tendon ID	Pos.	5mm		10mm		15mm		20mm		25mm		30mm		35mm	
		AP	TR	AP	TR	AP	TR	AP	TR	AP	TR	AP	TR	AP	TR
P1L	A	5.5	6.5	5.1	8.0	4.3	7.4	4.9	6.9	5.1	7.1	5.6	9.9	6.6	16.5
P1R	B	9.5	5.6	4.4	7.8	4.1	5.6	3.3	5.3	3.2	5.1	3.1	6.0	3.2	6.1
P2L	C	8.2	9.2	3.6	5.6	2.6	5.5	2.7	4.0	3.	6.5	2.9	6.5	3.6	11.2
P2R	D	5.1	10.1	5.1	9.4	3.4	7.1	3.1	7.2	3.4	7.2	3.6	7.5	3.2	8.0
P3L	E	6.0	8.7	5.0	8.6	4.2	7.3	4.0	5.8	3.7	7.4	2.7	7.7	3.2	8.6
P3R	F	3.9	5.3	3.9	4.4	4.0	4.4	2.5	4.4	3.0	5.3	3.6	7.8	3.8	10.2
P4L	A	4.7	4.7	4.6	3.9	4.2	4.4	3.7	4.6	3.6	5.2	3.9	5.7	4.5	9.4
P4R	B	6.3	14.5	5.3	6.8	4.2	5.4	2.9	3.9	3.3	4.7	4.2	4.7	4.9	6.6
P5L	C	5.3	9.0	4.1	10.9	4.5	5.5	3.7	4.9	2.8	6.8	3.0	8.3	3.5	10.0
P5R	D	3.0	5.1	2.8	4.0	2.5	4.9	2.1	4.8	2.7	7.0	3.4	9.1	3.1	11.0
P6L	E	4.4	7.0	3.8	6.8	3.0	5.6	2.9	5.1	2.7	7.0	3.4	9.1	3.1	11.0
P6R	F	6.5	9.3	6.6	9.6	5.0	8.5	3.2	5.7	2.5	6.1	2.5	6.3	2.1	7.3
P7L	A	5.1	10.5	5.2	9.1	4.7	9.5	3.3	9.9	3.6	12.6	3.6	13.4	3.5	10.9
P7R	B	5.8	7.3	4.8	6.0	5.2	5.3	3.3	4.4	4.6	5.9	5.4	7.7	6.0	11.4
P8L	C	3.9	6.4	5.1	5.4	3.1	3.6	2.4	3.7	2.1	5.0	1.8	8.7	3.4	8.6
P8R	D	4.1	6.6	4.0	5.8	3.1	4.8	3.1	5.5	2.0	8.4	4.3	6.9	4.3	7.6
P9L	A	3.4	7.2	3.8	7.5	4.0	5.5	3.0	4.0	3.1	4.4	3.8	5.3	4.0	6.7
P9R	B	4.7	4.7	3.7	4.9	2.4	4.8	2.6	4.0	2.6	3.5	3.2	3.6	3.5	10.5
P10L	C	5.1	8.1	5.0	6.5	4.5	6.4	4.6	6.6	4.4	7.6	4.3	6.7	4.0	6.9
P10R	D	3.1	4.2	3.0	4.4	3.4	3.2	2.5	3.5	3.0	3.1	2.8	4.7	3.2	7.8

**Table 7:** Magnetic Resonance Imaging (MRI) Results for All tendons

Tendon ID	Position	Sequence T1			Sequence PD			Sequence T2		
		AP	TR	OD	AP	TR	OD	AP	TR	OD
P5L	C			107	2.9	3.9	163			154
P6R	F			123	2.8	3.6	223			165
P10R	D			112	4.3	3.2	142			144
P1L	D			460	4.0	4.7	780			215
P2R	A			217	2.4	4.4	353			213
P3L	B			145	2.0	4.4	393			348
P1R	E			179	2.4	2.5	201			180
P2L	F			165	2.0	2.8	181			150
P10L	C			134	2.1	2.9	181			176
P5R	D			131	2.0	3.1	168			205
P6L	E			172	2.4	2.6	251			276
P3R	C			155	2.8	3.0	211			167

**Table 8:** Bone Mineral Density (BMD) Results for All Tendons

Tendon ID	Group	BMD (g/cm <sup>2</sup> )
P5L	1	0.353
P6R	1	0.394
P10R	1	0.356
P1L	2	0.347
P2R	2	0.349
P3L	2	0.351
P1R	3	0.405
P2L	3	0.439
P10L	3	0.347
P5R	3	0.365
P6L	3	0.395
P3R	3	0.347

\*Group 1 - Degenerated, Group 2 - Degenerated & Punched, and Group 3 - Contralateral.

Note: Not all values in Tables 6-8 were used in this study as some were not considered valid. The following tables include the subsets of data used in this study.

**Table 9:** Ultrasound results for subset of valid tendons (T = healing time in weeks)

Tendon ID	Group*	T	5mm		10mm		15mm		20mm		25mm		30mm		35mm	
			AP	TR	AP	TR	AP	TR	AP	TR	AP	TR	AP	TR	AP	TR
P5L	1	2	5.3	9.0	4.1	10.9	4.5	5.5	3.7	4.9	2.8	6.8	3.0	8.3	3.5	10.0
P6R	1	4	6.5	9.3	6.6	9.6	5.0	8.5	3.2	5.7	2.5	6.1	2.5	6.3	2.1	7.3
P10R	1	4	3.1	4.2	3.0	4.4	3.4	3.2	2.5	3.5	3.0	3.1	2.8	4.7	3.2	7.8
P1L	2	2	5.5	6.5	5.1	8.0	4.3	7.4	4.9	6.9	5.1	7.1	5.6	9.9	6.6	16.5
P2R	2	4	5.1	10.1	5.1	9.4	3.4	7.1	3.1	7.2	3.4	7.2	3.6	7.5	3.2	8.0
P5R	3	2	3.0	5.1	2.8	4.0	2.5	4.9	2.1	4.8	2.7	7.0	3.4	9.1	3.1	11.0
P3R	3	4	3.9	5.3	3.9	4.4	4.0	4.4	2.5	4.4	3.0	5.3	3.6	7.8	3.8	10.2
P6L	3	4	4.4	7.0	3.8	6.8	3.0	5.6	2.9	5.1	2.7	7.0	3.4	9.1	3.1	11.0

\*Group 1 - Degenerated, Group 2 - Degenerated & Punched, and Group 3 - Contralateral.

**Table 10:** Magnetic resonance imaging (MRI) results for subset of valid tendons

Tendon ID	Position	Group*	Healing Time	Sequence T1			Sequence PD			Sequence T2			Cross-sectional Area (m <sup>2</sup> )
				AP	TR	OD	AP	TR	OD	AP	TR	OD	
P5L	C	1	2 Weeks	-	-	107	2.9	3.9	163	-	-	154	17.5
P6R	F	1	4 Weeks	-	-	123	2.8	3.6	223	-	-	165	17.6
P10R	D	1	4 Weeks	-	-	112	4.3	3.2	142	-	-	144	19.1
P1L	D	2	2 Weeks	-	-	460	4.0	4.7	780	-	-	215	92.1
P2R	A	2	4 Weeks	-	-	217	2.4	4.4	353	-	-	213	30.1
P5R	D	3	2 Weeks	-	-	131	2.0	3.1	168	-	-	205	11.8
P3R	C	3	4 Weeks	-	-	155	2.8	3.0	211	-	-	167	11.2
P6L	E	3	4 Weeks	-	-	172	2.4	2.6	251	-	-	276	14.1

\*Group 1 - Degenerated, Group 2 - Degenerated & Punched, and Group 3 - Contralateral.

**Table 11:** Bone mineral density (BMD) results for subset of valid tendons

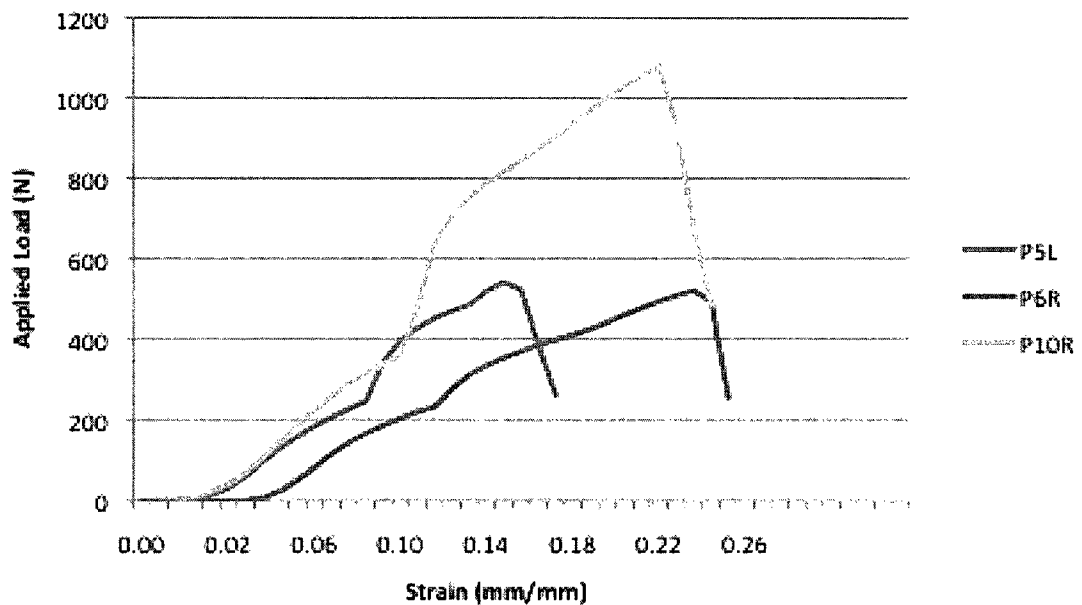
Tendon ID	Group		BMD (g/cm <sup>2</sup> )
P5L	1	2 Weeks	0.353
P6R	1	4 Weeks	0.394
P10R	1	4 Weeks	0.356
P1L	2	2 Weeks	0.347
P2R	2	4 Weeks	0.349
P5R	3	2 Weeks	0.365
P3R	3	4 Weeks	0.347
P6L	3	4 Weeks	0.395

\*Group 1 - Degenerated, Group 2 - Degenerated & Punched, and Group 3 - Contralateral.

## C.2 Mechanical Testing Results

**Table 12:** Mechanical strength of Group 1 (Degenerated) tendons

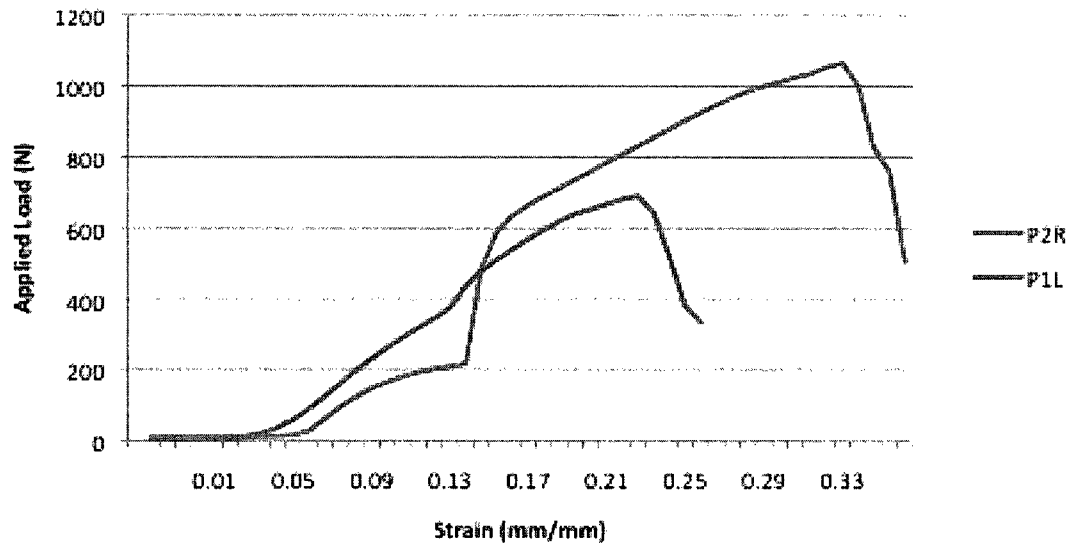
Tendon ID	Harvest Time	Failure Load (N)	Mean Stress (MPa)
P5L	2 Weeks	543	31.1
P6R	4 Weeks	522	29.7
P10R	4 Weeks	1081	56.5



**Figure 31:** Load vs. displacement plot for Group 1 (Degenerated) tendons.

**Table 13:** Mechanical strength of Group 2 (Degenerated & Punched) tendons

Tendon ID	Harvest Time	Failure Load (N)	Mean Stress (MPa)
P1L	2 Weeks	690	7.5
P2R	4 Weeks	1066	35.4

**Figure 32:** Load vs. displacement plot for Group 2 (Degenerated & Punched) tendons.**Table 14:** Mechanical strength of contralateral tendons

Tendon ID	Harvest Time	Failure Load (N)	Mean Stress (MPa)
P5R	2 Weeks	1087	92.1
P3R	4 Weeks	623	55.7
P6L	4 Weeks	740	52.6

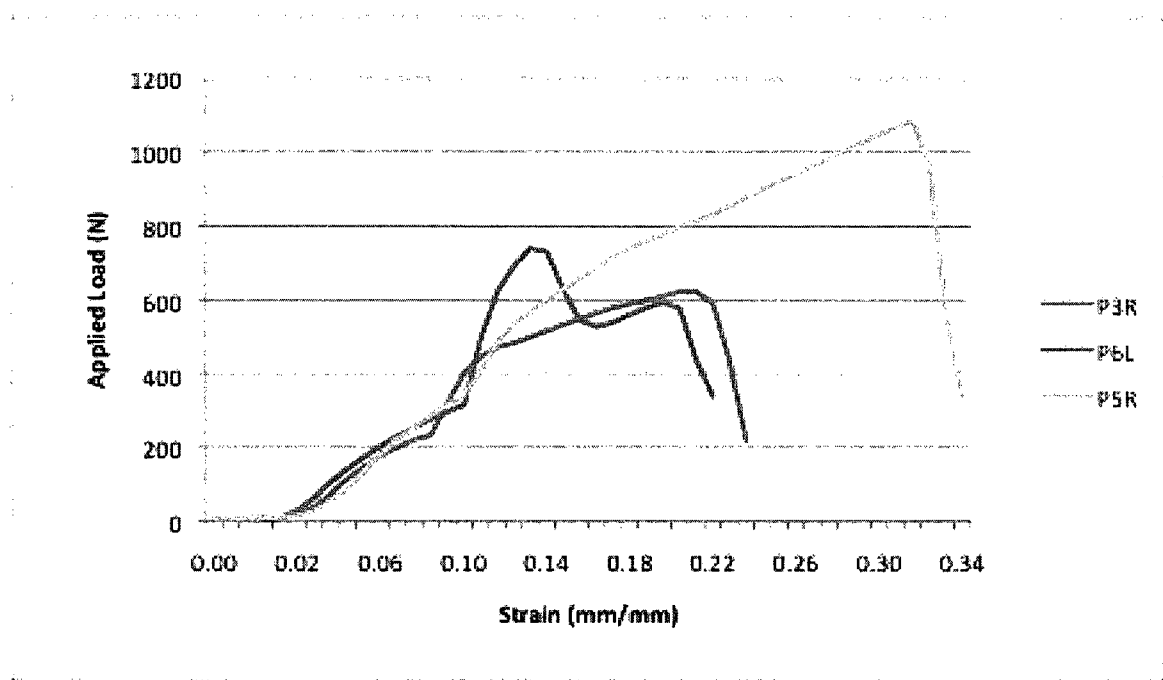


Figure 33: Load vs. displacement plot for contralateral Tendons.

## Appendix D

### Previous Healthy-Injured Study Results

#### D.1 Imaging Results

**Table 15:** Previous Interval Study: Clinical imaging data for healthy rabbit Achilles tendons and for control tendons immediately after creation of a full-thickness antero-posterior large defect [1]

		Group	Week		
			0	4	8
MRI	Muscle volume (mL)	Experimental	27.6 ± 2.2	27.9 ± 0.7	27.9 ± 2.2
		Control	26.4 ± 0.7	27.8 ± 0.7	28.3 ± 2.1†
	Anteroposterior diameter (mm)	Experimental	2.3 ± 0.2	4.6 ± 0.8*†	3.9 ± 0.5*††
		Control	2.4 ± 0.2	2.4 ± 0.2	2.3 ± 0.2
	Mediolateral diameter (mm)	Experimental	4.0 ± 0.5	5.7 ± 0.8*†	4.9 ± 0.3*††
		Control	4.2 ± 0.3	4.4 ± 0.4	4.3 ± 0.4
	Cross-sectional Area (mm <sup>2</sup> )	Experimental	6.6 ± 1.7*	18.9 ± 5.0*†	14.3 ± 1.5*††
		Control	9.0 ± 1.4	9.3 ± 0.8	7.8 ± 1.1†
	T1 Weighted OD	Experimental	149 ± 15	256 ± 53*†	184 ± 24*†
		Control	147 ± 18	158 ± 20	152 ± 20
	PD OD	Experimental	187 ± 29	400 ± 122*†	287 ± 56*††
		Control	182 ± 29	170 ± 31	187 ± 25
T2 Weighted OD	Experimental	174 ± 18	200 ± 14*†	208 ± 26*†	
	Control	182 ± 24	180 ± 15	182 ± 20	
US	Anteroposterior diameter (mm)	Experimental	3.5 ± 0.4	4.9 ± 0.7*†	4.6 ± 0.4*†
		Control	3.6 ± 0.3	3.5 ± 0.4	3.7 ± 0.3
BMD	Calcaneus (g/cm <sup>3</sup> )	Experimental	0.34 ± 0.03	0.36 ± 0.02	0.37 ± 0.02
		Control	0.32 ± 0.03	0.35 ± 0.02	0.36 ± 0.04†

All data are expressed as mean ± 1 standard deviation. N = 10 in all cases Except control group at 4 weeks (n = 8). P < 0.05 for difference from contralateral tendons (\*), from 0 weeks (†) and from 4 weeks (‡).

**Table 16:** Previous Longitudinal Study: Clinical imaging data for healthy rabbit Achilles tendons and for control tendons immediately after creation of a full-thickness anteroposterior oval defect and up to 16 weeks after surgery [1]

		Group	Week							
			0	1	2	4	6	8	10	16
MRI	Anteroposterior diameter (mm)	Experimental	2.3	3.3	3.9	3.4	3.0	3.6	3.6	4.1
		Control	-	2.3	2.5	2.3	2.5	2.3	2.5	2.4
	Mediolateral diameter (mm)	Experimental	3.0	4.9	6.3	4.5	5.3	4.5	4.9	4.4
		Control	-	4.0	4.2	3.8	3.8	3.9	4.4	4.7
	Cross-sectional Area (mm <sup>2</sup> )	Experimental	8.2	12.0	20.0	15.7	14.1	13.4	13.0	12.5
		Control	-	7.5	8.8	7.8	7.8	8.6	7.8	7.9
	T1 Weighted OD	Experimental	169	302	256	186	159	131	117	147
		Control	-	116	126	104	130	136	65	163
	PD OD	Experimental	101	883	447	325	235	191	151	180
		Control	-	145	108	93	102	107	115	174
	T2 Weighted OD	Experimental	210	442	130	147	110	118	116	180
		Control	-	115	129	90	120	129	160	132
US	Anteroposterior diameter (mm)	Experimental	3.6	5.3	5.5	4.0	4.3	4.4	4.7	4.6
		Control	-	3.8	4.0	3.7	3.2	3.3	3.8	3.9
BMD	Calcaneus (g/cm <sup>3</sup> )	Experimental	NA	0.33	0.35	0.32	0.36	0.32	0.34	0.39
		Control	-	0.33	0.35	0.32	0.36	0.32	0.34	0.38

N = 1 in all cases. NA = not available.

## D.2 Mechanical Testing Results

**Table 17:** Previous Interval Study: Mechanical properties of healthy rabbit Achilles tendons after an acute partial tendon defect [1]

Week	Group	Peak load (N)	Stress (MPa)	Stiffness(N/mm)
0	Experimental	332 ± 128*	50 ± 16*	156 ± 37
	Control	764 ± 171	85 ± 17	140 ± 39
4	Experimental	712 ± 106†	39 ± 9*	108 ± 34†
	Control	717 ± 159	77 ± 16	140 ± 31
8	Experimental	836 ± 90†‡	58 ± 6*‡	116 ± 13†
	Control	727 ± 180	94 ± 26	127 ± 24

All data are expressed as mean ± 1 standard deviation. P < 0.05 for difference from contralateral tendons (\*), from 0 weeks (†) and from 4 weeks (‡).

**Table 18:** Previous Longitudinal Study: Mechanical properties of healthy Rabbit Achilles tendons after an acute partial tendon defect [1]

Week	Group	Peak load (N)	Stress (MPa)	Stiffness(N/mm)
0	Experimental	387	47	104
1	Experimental	424	35	170
	Control	604	80	92.1
2	Experimental	681	34	142
	Control	788	90	126
4	Experimental	787	50	108
	Control	711	91	121
6	Experimental	892	63	115
	Control	692	89	92
8	Experimental	644	48	155
	Control	766	89	108
10	Experimental	902	69	122
	Control	813	104	108
16	Experimental	984	79	139
	Control	1030	130	NA

N = 1 in all cases.

## D.3 Correlations Between Imaging and Mechanical Results

**Table 19:** Previous Study: Correlation between imaging outcome measures and mechanical measures 4 and 8 weeks after surgery [1]

Mechanical Measure	MR Imaging						US	BMD
	Antero-posterior diameter	Medio-lateral diameter	Cross-sectional area	T <sub>1</sub> -weighted OD	PD OD	T <sub>2</sub> -weighted OD	Antero-posterior diameter	
Peak load	-0.15	-0.29	-0.28	-0.46*	-0.39	-0.09	-0.20	0.30
Stiffness	-0.24	-0.10	-0.22	-0.40	-0.37	0.10	-0.21	0.03
Stress	-0.70*	-0.67*	-0.83*	-0.73*	-0.69*	-0.02	-0.33	0.62*

\*P < 0.05.

Note: The correlation between stress and tendon dimensions (anterolateral diameter, mediolateral diameter and cross-sectional area) are redundant since dimensions enter into the calculation of stress.